International Journal of
Molecular Sciences

MDPI

Article

Sex Difference in Cardioprotection against Acute Myocardial Infarction in MAO-B Knockout Mice In Vivo

Jacqueline Heger [1,*,†], Tamara Szabados [2,3,†], Paulin Brosinsky [1], Péter Bencsik [2,3], Péter Ferdinandy [3,4] and Rainer Schulz [1]

1 Institute of Physiology, Justus Liebig University, 35392 Giessen, Germany
2 Department of Pharmacology and Pharmacotherapy, University of Szeged, 6722 Szeged, Hungary
3 Pharmahungary Group, 6722 Szeged, Hungary
4 Department of Pharmacology and Pharmacotherapy, Semmelweis University, 1094 Budapest, Hungary
* Correspondence: jacqueline.heger@physiologie.med.uni-giessen.de
† These authors contributed equally to this work.

Abstract: The cardiomyocyte-specific knockout (KO) of monoamine oxidase (MAO)-B, an enzyme involved in the formation of reactive oxygen species (ROS), reduced myocardial ischemia/reperfusion (I/R) injury in vitro. Because sex hormones have a strong impact on MAO metabolic pathways, we analyzed the myocardial infarct size (IS) following I/R in female and male MAO-B KO mice in vivo. Method and Results: To induce the deletion of MAO-B, MAO-B KO mice (Myh6 Cre+/MAO-B$^{fl/fl}$) and wild-type (WT, Cre-negative MAO-B$^{fl/fl}$ littermates) were fed with tamoxifen for 2 weeks followed by 10 weeks of normal mice chow. Myocardial infarction (assessed by TTC staining and expressed as a percentage of the area at risk as determined by Evans blue staining)) was induced by 45 min coronary occlusion followed by 120 min of reperfusion. Results: The mortality following I/R was higher in male compared to female mice, with the lowest mortality found in MAO-B KO female mice. IS was significantly higher in male WT mice compared to female WT mice. MAO-B KO reduced IS in male mice but had no further impact on IS in female MAO-B KO mice. Interestingly, there was no difference in the plasma estradiol levels among the groups. Conclusion: The cardiomyocyte-specific knockout of MAO-B protects male mice against acute myocardial infarction but had no effect on the infarct size in female mice.

Keywords: monoamine oxidase B; mitochondria; ischemia/reperfusion

Citation: Heger, J.; Szabados, T.; Brosinsky, P.; Bencsik, P.; Ferdinandy, P.; Schulz, R. Sex Difference in Cardioprotection against Acute Myocardial Infarction in MAO-B Knockout Mice In Vivo. *Int. J. Mol. Sci.* **2023**, *24*, 6443. https://doi.org/10.3390/ijms24076443

Academic Editor: Peter Radermacher

Received: 13 February 2023
Revised: 22 March 2023
Accepted: 25 March 2023
Published: 29 March 2023

1. Introduction

Monoamine oxidase (MAO) is a protein located in the outer mitochondrial membrane [1], where it degrades neurotransmitters and biogenic amines. The oxidative deamination of primary, secondary and tertiary amines is coupled to the reduction in the covalently linked co-factor flavin adenine dinucleotide (FAD) [2]. With the aid of water and oxygen, the formation of aldehydes, ammonia and the reactive oxygen species (ROS) molecule hydrogen peroxide (H_2O_2) are formed in the mitochondrial matrix and in the cytosol of the cell [3–5]. FAD is thereby reduced to $FADH_2$; it accepts two hydrogen atoms and undergoes a net gain of two electrons. The recycling of FAD generates H_2O_2. The interaction of the FAD side chain with MAO-B is of utmost importance to incorporate FAD into MAO-B [6], because a deformation in the flavin ring negatively affects the reactive center and plays a crucial role for irreversible MAO inhibitor binding [7]. An accumulation of catecholamines can result in numerous diseases, such as Brunner syndrome [8], arrhythmia or general cardiovascular problems [9,10]. There are two isoforms of MAO, MAO-A and MAO-B, which are both strongly expressed in the heart [11,12]. They differ in their substrate specificity and inhibitor sensitivity. MAO-A primarily oxidizes serotonin and norepinephrine, while both MAO-A and MAO-B metabolize tyramine and dopamine. β-phenylethylamine (PEA) is a biogenic trace amine and a substrate for MAO-B [13,14].

Myocardial infarction (MI) occurs as a consequence of the prolonged interruption of the blood supply to the heart. If patients survive a severe MI, the heart function deteriorates, and heart failure (HI) often develops. While reperfusion through primary percutaneous coronary intervention is the only possibility to reduce myocardial infarct size, reperfusion itself induces further damage to the heart muscle, known as reperfusion injury [15,16].

Oxidative stress is a major contributor to irreversible ischemia/reperfusion (I/R) injury. Already during ischemia, the amount of ROS rises and increases further with the beginning of reperfusion. Apart from enzymes in the cytosol of the cell, ROS molecules are also generated by mitochondria [17]. Under stress conditions, such as I/R, the autonomic nervous system is activated, releasing neurotransmitters such as norepinephrine, which in turn are broken down by MAOs leading to the formation of H_2O_2, which can directly influence heart function [18].

Besides norepinephrine, serotonin (5-HT) and histamine also play important roles in I/R injury. 5-HT accumulates in the heart during ischemia and is degraded after reperfusion depending on the MAO-A activity after uptake into the cells [19]. Histamine co-localizes with norepinephrine in neurons [20] and is enclosed in cytoplasmatic granules of mast cells, which lie adjacent to blood vessels and between cardiomyocytes [21]. Mast cells become activated by I/R and release histamine [22] and histamine released from the heart is increased during I/R [21,23,24]. Histamine is metabolized to 1-N-Methylhistamine (1N-Met) which acts as a substrate for MAO-B, thereby increasing the ROS formation [24].

The MAO pattern in different cell types has been examined by the use of specific inhibitors, where MAO-A is inhibited by low concentrations of clorgyline and MAO-B by selegiline. Both isoforms are inhibited by pargyline [25]. MAOs play an essential role in the nervous system by modulating the levels of neurotransmitters. Various neurological diseases such as depression, Alzheimer's and Parkinson's are associated with altered MAO levels. The different preferences in substrate affinity are crucial for the different clinical significance of the two MAOs [26]. The inhibition of both isoforms or the use of irreversible MOA inhibitors can be fatal by the accumulation of MAO substrates, such as tyramine or serotonin. Increased amounts of tyramine can enter the systemic circulation and, from there, adrenergic neurons, consequently increasing the noradrenaline release and resulting in a severe hypertensive response [5,27]. Similarly, an increase in serotonin concentration might be deleterious, leading to serious adverse outcomes, including death [28]. Selective MAO-B inhibition might provide a cardiac benefit while MAO-A can maintain tyramine and serotonin homeostasis.

Besides experiments with MAO-specific inhibitors [29], MAO activity is inhibited by gene targeting in mice [13,30,31]. MAO-B inhibition prevented the doxorubicin-induced cardiac dysfunction [29]. We have previously shown that the cardiomyocyte-specific deletion of MAO-B is accompanied by a reduction in mitochondrial ROS production upon administration of specific substrates and infarct size and accelerated functional recovery following I/R in Landendorff-perfused male and female mice hearts in vitro [32].

Gender differences in cardiac I/R injury have already been described (for a review, see [33–36]. Such an increased resistance of female hearts to I/R in vivo and in vitro was reported for several species [33,37,38] and has been attributed to the potential cardioprotective mechanism(s) of estrogen [33]. Interestingly, females have higher plasma MAO activity than males [39] and estrogens can modulate MAO activity [40]. Women show a different susceptibility to diseases than men and react differently to treatment. The incidence of depression in women is nearly double that in men. Female susceptibility may be linked to surges in reproductive hormones [41]. Women had a statistically superior response to MAOIs as antidepressant treatment [42], demonstrated by elevated levels of serotonin, as well as the serotonin metabolite 5-hydroxyindoleacetic acid (5-HIAA), to be found in women compared to men [41]. This makes a study of females and males with MAO-B KO even more promising.

In the present study, we therefore wanted to 1. confirm our previous in vitro findings on the cardiomyocyte-specific deletion of MAO-B being cardioprotective in an in vivo

mice model of I/R injury and 2. compare the cardioprotective potential in female and male hearts.

2. Results

2.1. Cardiomyocyte-Specific MAO-B Deletion and Mortality Rate after I/R

There was no major difference in the mortality rate between the wild-type (WT) and cardiomyocyte-specific MAO-B knockout (KO) females or males, as well as in the WT females vs. KO females. However, comparing all the male to female mice, there was a tendency for a higher mortality rate in the males compared to the females ($p = 0.103$, when analyzed by Fisher's exact test) (Figure 1).

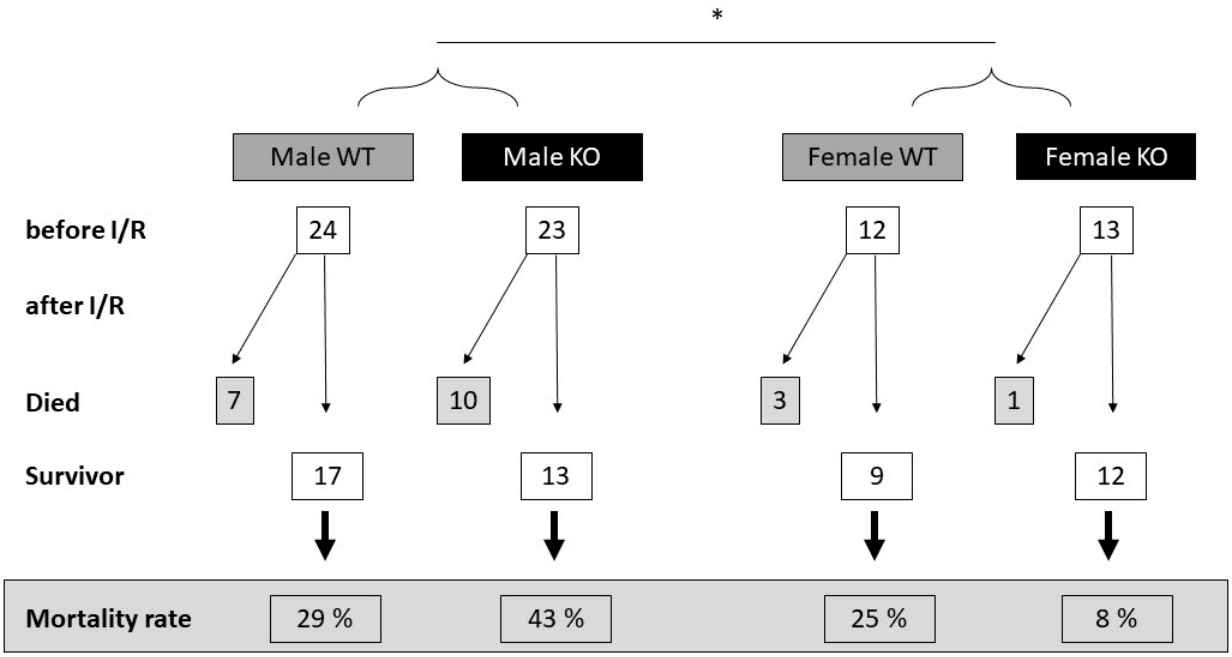

Figure 1. Higher mortality rate in male wild-type (WT) and cardiomyocyte-specific MAO-B knockout (KO) mice compared to female mice. WT and KO hearts were exposed to 45 min ischemia and 120 min reperfusion. Summary of the number of operated mice before and after surgery. Excluded mice had blood in the urine or surgery complications. There is no significant difference among groups when analyzed groups separately by Chi-square test or between WT and KO animals when analyzed by Fisher's exact test. However, there is a slightly decreasing tendency but not significant in all-cause mortality in female individuals as compared to males when analyzed by Fisher's exact test (* $p = 0.103$).

2.2. Cardiomyocyte-Specific MAO-B Deletion and Infarct Size

The WT male mice had a significantly higher infarct size than the WT female mice following 45 min ischemia and 120 min reperfusion. There was no significant difference in the area at risk between the different groups (Figure 2A). The cardiomyocyte-specific knockout of MAO-B (KO) reduced the myocardial infarct size in the male hearts but did not affect the infarct size in the female hearts (Figure 2B). Interestingly, the infarct size in the male KO was similar to that of both the WT and KO female hearts following I/R.

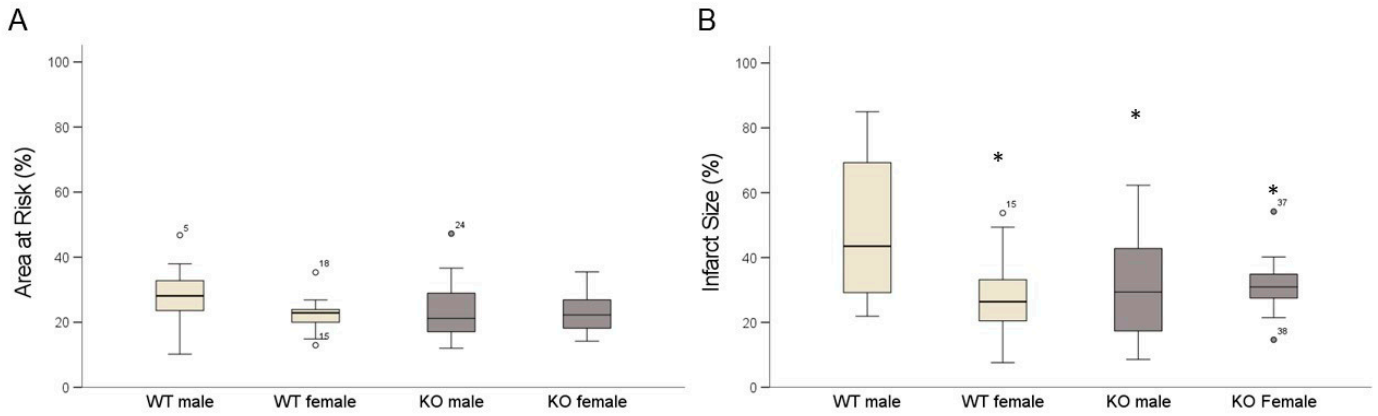

Figure 2. Male MAO-B KO mice benefit from MAO-B deletion regarding reduced size of infarcted area. (**A**) shows quantification of area at risk and (**B**) infarct size quantification. (WT male n = 14; WT female n = 9; KO male n = 11; KO female n = 11). Data are represented as box plots expressing median, 25% and 75% quartiles, upper and lower whisker and outliers. * $p < 0.05$ WT male vs. WT female, KO male, KO female, Student's *t*-test.

2.3. Cardiomyocyte-Specific MAO-B Deletion and Heart Rate

After reperfusion, the female WT as well as the male and female KO mice responded with a significant increase in heart rate. Only the WT male hearts did not show an increase in heart rate (Figure 3).

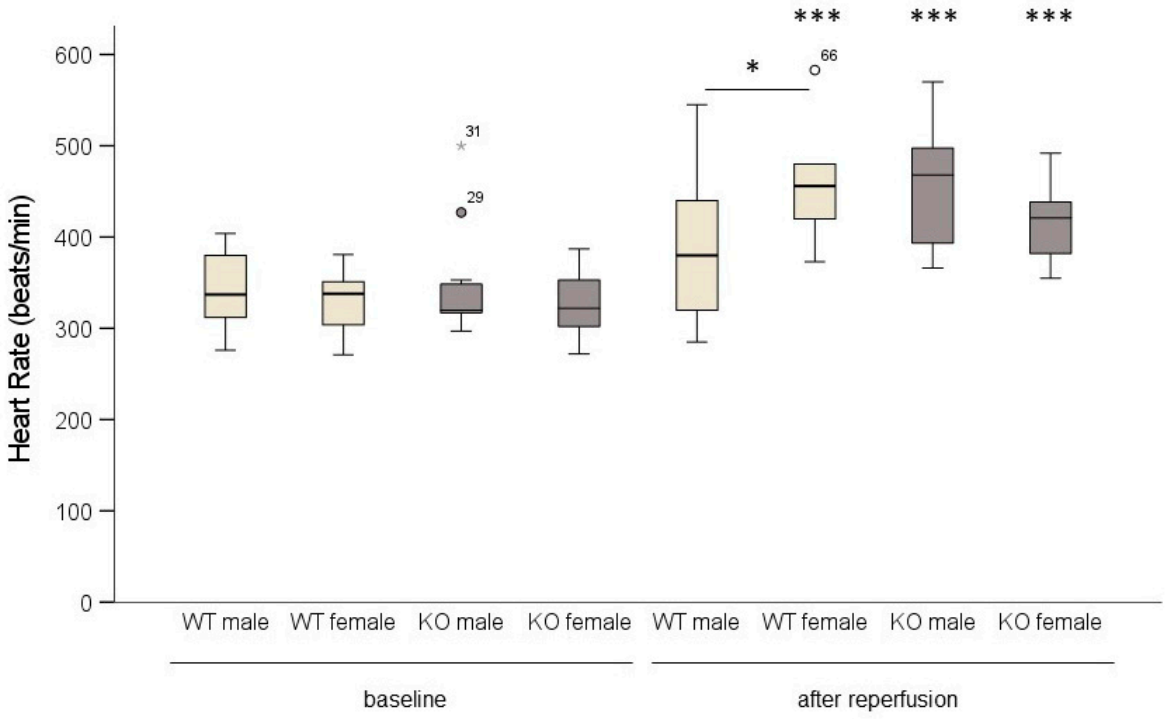

Figure 3. In male wild-type (WT) mice, heart rate did not increase following ischemia/reperfusion. WT and cardiomyocyte-specific MAO-B knockout (KO) hearts were exposed to 45 min ischemia and 120 min reperfusion. Heart rate was measured baseline and after reperfusion. (WT male n = 14; WT female n = 9; KO male n = 11; KO female n = 11). Data are represented as box plots expressing median, 25% and 75 % quartiles, upper and lower whisker and outliers (○,⋆). * $p < 0.05$, *** $p < 0.001$ baseline vs. after reperfusion, Student's *t*-test. Two-way ANOVA: $p < 0.001$, baseline vs. after reperfusion $p < 0.001$, genotype * sex $p = 0.02$.

In addition, the differences in the number of reperfusion arrhythmias were measured among the different groups (Figure 4). The incidence and severity of the arrhythmias were evaluated according to convention 23 of the Lambeth conventions II [43]. The male mice displayed more severe arrhythmias than the females as evaluated by the arrhythmia score. The arrhythmia score was calculated according to the phenotype and duration of the arrhythmias. The ventricular premature beats (1), ventricular bigeminy (2) and ventricular salvos (3) were scored; however, neither ventricular tachycardia nor fibrillation occurred in any of the individuals. The duration of the arrhythmias was expressed in minutes. In the cases where several occurrences of different types of arrhythmias were found in one individual, the most severe arrhythmia with the longest duration was used for the analysis. The data are expressed as a violin plot and analyzed by the Kruskal–Wallis test (four groups) as well as by Mann–Whitney non-parametric tests (when the difference between the males and females was tested). The Mann–Whitney test resulted in only a decreasing tendency in the WT female mice as compared to the KO male mice ($p = 0.054$). However, when the WT and KO males as well as the WT and KO females were united, the Mann–Whitney test showed a significantly decreased arrhythmia score in the female mice as compared to the males ($p = 0.014$), regardless of gene modification.

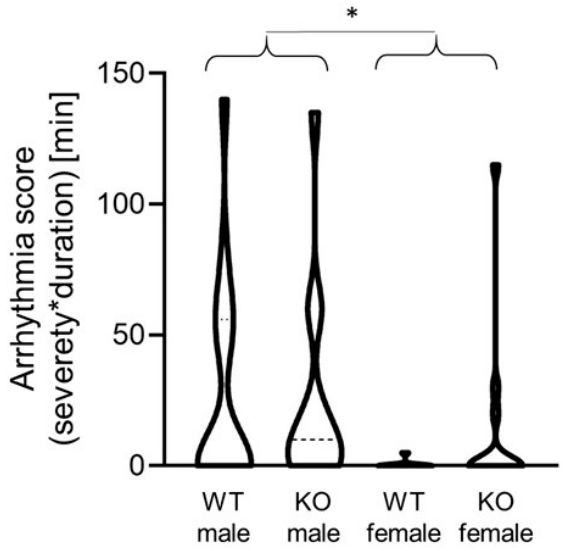

Figure 4. Violin plot representing the severity and duration of reperfusion arrhythmias. (WT male, male wild-type mice; KO male, male MAO-B knockout mice; WT female, female wild-type mice; KO female, female MAO-B knockout mice). * $p = 0.014$ when WT and KO males are compared to WT and KO females as analyzed by Mann–Whitney test.

2.4. Cardiomyocyte-Specific MAO-B Knockout and Heart Weight

The female mice had reduced heart weights (HW) and body weights (BW) compared to the male mice (Figure 5A,B). The HW/BW ratios were similar in the WT males and females (Figure 5C) as well as in the male cardiomyocyte-specific knockout (KO) mice, while in the female KO mice the HW/BW ratio was reduced compared to the male mice.

2.5. Cardiomyocyte-Specific MAO-B Knockout and 17β Estradiol

As estradiol might affect I/R injury and MAO activity, 17β estradiol levels were measured (Table 1). The male MAO-B KO had similar estradiol levels as the WT as well as the KO females. In contrast, the WT males had significantly higher estradiol levels compared to all other groups.

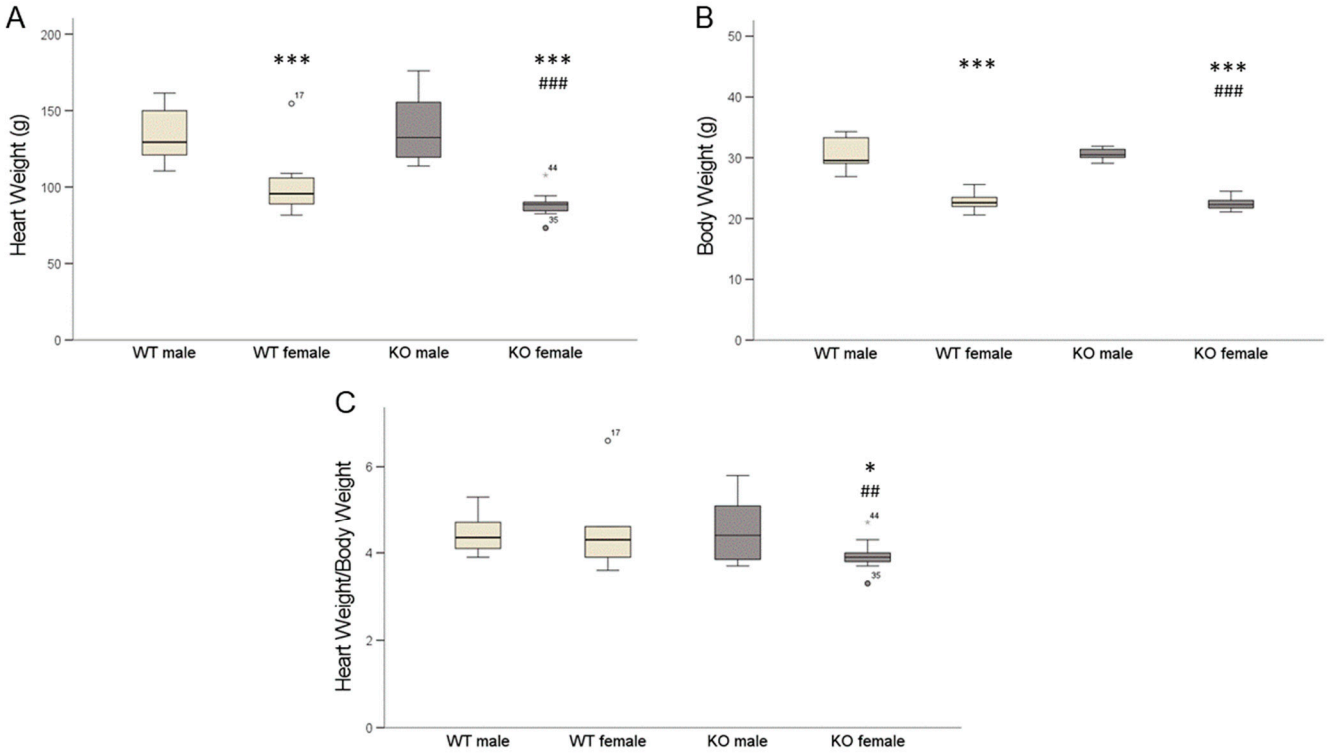

Figure 5. Heart weight (HW) and body weight (BW) as well as HW/BW ratios of mice. Female mice had reduced heart weight (**A**), *** $p < 0.001$ male vs. female and ### $p < 0.001$ WT male vs. KO female, Student's *t*-test; two-way ANOVA: sex $p < 0.001$. Female mice had reduced body weight (**B**) compared to male mice, *** $p < 0.001$ male vs. female, ### $p < 0.001$ WT male vs. KO female, Student's *t*-test; two-way ANOVA: sex $p < 0.001$. HW/BW ratios (**C**) were similar in WT males and females as well as in male cardiomyocyte-specific knockout (KO) mice, while in female KO mice HW/BW ratio was reduced, * $p < 0.05$ KO male vs. KO female and ## $p < 0.01$ WT male vs. KO female, Student's *t*-test. Two-way ANOVA: sex * genotype $p = 0.088$. (WT male n = 14; WT female n = 9; KO male n = 11; KO female n = 11). Data are represented as box plots expressing median, 25% and 75 % quartiles, upper and lower whisker and outliers (○,⋆).

Table 1. Plasma 17β estradiol levels in WT and MAO-B KO mice. WT and MAO-B KO hearts were exposed to ischemia for 45 min and reperfusion for 120 min. Plasma samples were collected and 17β estradiol levels determined. * $p < 0.05$ WT male vs. WT female, ## $p < 0.01$ WT male vs. MAO-B KO male and female, Student's *t*-test. Two-way ANOVA: genotype $p = 0.005$; sex $p = 0.161$.

	WT		**MAO-B KO**	
	Male	**Female**	**Male**	**Female**
Mean	27.9 *,##	25.1	23.7	23.9
SEM	0.81	0.96	1.01	0.81
N	9	9	8	11

3. Discussion

Female WT are more resistant to I/R injury and develop a smaller infarct size after I/R compared to male WT mice. The cardiomyocyte-specific knockout of MAO-B reduced IS in male mice but had no (additive) protective effect in female mice. Protection by estrogen may be due to altered gene expression.

Sex difference in I/R injury: Estradiol can protect the heart against ischemia-induced injury by blocking the mitochondrial permeability transition pore (MPTP) opening [44]. Moreover, estrogens can preserve cardiac function after I/R by diminishing cytokine

levels [45]. In women with estrogen therapy because of depression, estradiol decreases the expression of MAO-A and MAO-B through the interaction with its intracellular receptors [46]. Estradiol binds to different estrogen receptors (ER) (ER-α and ER-β) or a G-protein-coupled estrogen receptor (GPR30 or GPER) [47], which can thereby regulate various physiological and pathological processes [48]. ER-β localizes to mitochondria, thereby modulating the mitochondrial calcium influx, ATP production, apoptosis and free radical species formation, all processes critically involved in I/R injury [49] (for a review, see [36]).

Thus, although estradiol is important for I/R injury, there was no evidence of an increase in circulating plasma 17β-estradiol concentrations and cardioprotection in the different groups of mice in the present study. It is possible that the timing of the sampling is not appropriate or that 17β estradiol has already been internalized in a receptor-bound manner. In addition, Klaiber et al. [50] reported that mean values of serum estradiol levels in men with myocardial infarction were significantly elevated over the comparable mean values of a respective control group. Estrogens can increase adrenergic activity, which would increase myocardial oxygen demand, and testosterone can be converted to estradiol by aromatase in muscles.

Testosterone increases the gene expression of enzymes such as MAO through the direct activation of androgen receptors (AR) [51]. During I/R, AR increase in males as compared to females, leading to increased cardiac injury via the activation of apoptosis [52]. We did not measure the testosterone levels or AR in the present study, but in our previous study [32], the infarct size did not differ between male and female hearts, making such an explanation unlikely.

Apart from sex hormones, differences are found in the regulation of the cell survival pathways in males and females [16]. Cardioprotection in female rats after I/R is mediated by altered mitochondrial enzyme activity that encompasses a phosphoinositide-3-kinase (PI3K)-mediated reduction in ROS generation and a better removal of ROS by-products [37]. Interestingly, females have increased activity of aldehyde dehydrogenase 2 (ALDH2) [37]. MAOs degrade neurotransmitters and biogenic amines which, in addition to the production of ROS, also leads to the formation of aldehydes [3,4]. ALDH2 inactivates aldehydes in the heart [53] and ALDH2 activation before an ischemic event decreased the infarct size [54]. ALDH2 is located in the mitochondria and is important for the detoxification of 4-hydroxy-2-nonenal (4-HNE), which is produced during oxidative stress [55,56]. The downregulation of ALDH2 in cardiomyocytes by siRNA impaired the mitochondrial function demonstrated by a reduction in the mitochondrial membrane potential [57]. The overexpression of ALDH2 protects against 4-HNE accumulation and cardiac dysfunction in transgenic mice with the cardiac overexpression of MAO-A [56]. However, the aldehyde intermediates generated by MAO-B may also contribute to the alteration of the mitochondrial function [57]. Thus, an altered expression of ALDH2 could be important for the gender-specific cardioprotection against I/R. A possible approach to investigate the importance of gender, MAO-B and ALDH2 in the context of I/R injury would be the use of a MAO-B-specific inhibitor in ALDH2-overexpressing mice [58]. The use of MAO inhibitors could lead to an additive effect, thereby confirming the gender difference. If the cardioprotective effect in females is due to the increased activity of ALDH2, no difference should be seen between ALDH2-overexpressing mice with and without MAO inhibition. However, these experiments would completely go beyond the scope of this work.

Mortality and infarct size: It is well established that an increased infarct size is associated with increased mortality. Thus, the reduced mortality in WT female mice as compared to WT male mice is in accordance with this assumption. However, while the infarct size was reduced by the cardiomyocyte-specific knockout of MAO-B in male mice, the mortality rate remained high. Although the extent of reperfusion-induced arrhythmias was reduced, the latter potentially being explained by the desensitization of β-adrenoceptors. Wang et al. [59] discovered that MAOs desensitize the β_1-adrenergic pathway in mice injected intraperitoneally with the β-agonist isoproterenol to induce heart failure (HF). The

inhibition of MAO-A in isolated adult cardiomyocytes of HF hearts salvaged the signaling pathway and led to the activation of the protein kinase A [60]. Thus, more studies are needed to explain the differences in the mortality rate between cardiomyocyte-specific MAO-B knockout male and female mice following I/R.

Overall, it can be concluded that a cardiomyocyte-specific reduction in MAO-B contributes to cardioprotection in male but not in female mice. MAOs can be regulated by sex, but a detailed analysis of sex hormones influences on cell survival signaling pathways in a MAO-dependent manner remains to be elucidated.

4. Materials and Methods

4.1. Animals

All animals were housed in individually ventilated cages (Sealsafe IVC system, Tecniplast S.p.a., Buguggiate, Italy), which conform to the size recommendations in the most recent Guide for the Care and Use of Laboratory Animals DHEW (NIH Publication No. 85–23, revised 1996) and EU Guidelines 63/2010. Litter material placed beneath the cage was changed at least once a week. The animal room was temperature controlled having a 12-h light/dark cycle with lights on at 7 a.m. to 7 p.m., and was kept clean and vermin free. All animal experiments conformed to the EU directive about the care and use of laboratory animals, published by the European Union (2010/63/EU), and it was approved by the National Scientific Ethical Committee on Animal Experimentation (approval ID: XXVIII./171/2018.; on 24 January 2018). Generation of cardiac-specific and tamoxifen-inducible double-transgenic MAO-B KO mice (Myh6-MCreM_x_MAO-$B^{fl/fl}$) was described previously [33]. Preliminary sample size was calculated (https//:www.sample-size.net, accessed on 22 May 2020). The values were set up in case of females to $\alpha = 0.22$ (type I error rate); $\beta = 0.44$ (type II error rate); $P_0 = 0.15$ (Group 0 risk); $P_1 = 0.4$ (Group 1 risk); sample size = 12. The values were set up in case of males to $\alpha = 0.22$ (type I error rate); $\beta = 0.44$ (type II error rate); $P_0 = 0.2$ (Group 0 risk); $P_1 = 0.38$ (Group 1 risk); sample size = 24.

4.2. Genotyping

Ear biopsies were digested in 150 µL "Direct PCR Tail reagent" (#31-101-T, Peqlab [VWR, Darmstadt, Germany]) supplemented with 3 µL Proteinase K (20 mg/mL) and 150 µL H_2O at 55 °C for seven hours. Afterward, samples were incubated for 45 min at 85 °C. Samples were shortly centrifuged and supernatant was temporarily stored at 4 °C for subsequent PCR. Homozygous, heterozygous and wild-type mice were identified using the following primers:

MAO-$B^{fl/fl}$ forward	5′-GCC CAC GAG TAA GTA AAT ACG TGG A-3′
MAO-$B^{fl/fl}$ reverse	5′ GGT CTC TGT TTC TGG GAC AGT CTG-3
Myh6-MCreM forward	5′-GAC CAG GTT CGT TCA CTC ATG G-3′
Myh6-MCreM revererse	5′-AGG CTA AGT GCC TTC TCT ACA C-3′

PCRs were performed with Taq-polymerase-kit (#10342046, Invitrogen [Thermo Fisher Scientific, Miami, OK, USA]) with a MyCycler thermal cycler (BioRad, Feldkirchen, Germany). For Myh6-MCreM, annealing temperatures of 55 °C, 35 cycles were used, and for MAO- $B^{fl/fl}$, 62 °C, 34 cycles were used. Bands were detected with Gelred (Biotium, Fremont, CA, USA) in a 2% agarose gel after 45 min run in 1x TBE. Amplification of genomic DNA resulted in PCR products of either 226 bp or 353 bp. Presence of both products identifies heterozygous mice, 353 bp product homozygous mice and 226 bp product wild-type mice.

4.3. Determination of Infarct Size In Vivo

Briefly, Evans blue was injected in vivo into the apex of the left ventricle after re-occlusion of the coronary artery. Evans blue colors the whole left ventricle excluding the

area supplied by the occluded coronary artery to dark blue, thereby demarcating the area at risk. In the next step, the heart is excised and cut into 5 to 6 slices and incubated in vitro with 1% TTC at 37 °C. TTC binds to the reduced coenzymes such as NADH and FADH2 produced by the surviving cells, which leads to the conversion of TTC to a formazan dye and changes its color to red. Red-colored area is then identified as the surviving area inside the area at risk. Unstained pale areas are identified as infarct size. In detail: The mice were anesthetized by intraperitoneal (90 mg/kg i.p.) injection of sodium pentobarbital (Repose 50%, Le Vet. Pharma, Oudewater, The Netherlands) and were mechanically ventilated via tracheal cannula using room air (Model 845, Minivent, Harvard Apparatus, Holliston, MA, USA) in a volume of 150–200 µL and frequency of 140–150 strokes/min according to the recommendation of the ventilator's manufacturer. A left parasternal thoracotomy was performed, and the intercostal muscles were opened in the region of the 4th intercostal space. The pericardium was opened, and the left descending coronary artery (LAD) was occluded at its middle portion using an 8–0 synthetic, monofilament, non-absorbable polypropylene suture (Prolene®, Ethicon, Johnson & Johnson Kft Hungary, Budapest, Hungary) and a 3 cm piece of PE50 cannula to form a snare. For coronary artery occlusion, the plastic tubing was pressed onto the surface of the heart directly above the coronary artery and released for reperfusion. Myocardial infarction was induced by 45 min coronary occlusion followed by 120 min of reperfusion. Surface-lead ECG (Haemosys, Experimetria Inc., Budapest, Hungary) and body core temperature were monitored throughout the experiments to ensure the stability of the preparation. The successful induction of ischemia was visible as a pale coloring of the myocardium as well as changes in the ECG (ST-elevation, broadening of the QRS complex). At the end of the 120 min reperfusion, coronary artery was re-occluded, a maximum of 0.5 mL blood was collected by apical puncture of the left ventricle and gentle suction into a 1 mL syringe and immediately into Li-heparin tubes for plasma separation. Blood samples were centrifuged at 1000× *g* for 15 min at 4 °C, plasma was separated and immersed immediately into liquid nitrogen and stored at −70 °C until biochemical analysis. The heart was excised from the chest, the occlusion was released and atria and right ventricle were removed. The left ventricle was quickly frozen at −20 °C for 10 min and then cut into 1 mm thick slices. Infarct size was determined by standard 2,3,5-triphenyltetrazolium chloride (TTC) staining (1% for 10 min at 37 °C). Stained heart slices were put between two thin sheets of glass, and then photographed using a digital zoom camera (Canon Powershot SX60HS, Canon, Tokyo, Japan). Digital heart images were processed (both surfaces of the slices were merged into one image) and infarct size was evaluated by planimetry using InfarctSize™ v.2.5 software (developed by Pharmahungary, Budapest, Hungary) and expressed as a percentage of the area at risk [61].

4.4. Determination of 17 β Estradiol

Plasma samples were taken at the end of reperfusion period (at 120 min) just before intracardiac injection of Evans blue. The 17 β estradiol measurements were performed by using 17 beta Estradiol ELISA Kit (ab108667) of abcam (Cambridge, UK). The test was performed according to the manufacturer's instructions using plasma samples of mice after I/R.

4.5. Statistical Analysis

Statistical analysis was performed using SPSS (IBM SPSS Statistics 29). Results are represented as box plots and expressing median, 25% and 75% quartiles, upper and lower whisker and outliers as well as a violin plot for displaying reperfusion arrhythmias. The difference between two groups was compared using a two-tailed unpaired *t*-test. Comparison between more than two groups was performed with two-way ANOVA.

A one-way ANOVA, Kruskal–Wallis, Mann–Whitney and Student's *t*-test were used for the further evaluation of differences between two means. Values of $p < 0.05$ were considered to be statistically significant.

Author Contributions: Conceptualization, J.H. and R.S.; methodology, P.B. (Péter Bencsik) and T.S.; validation, P.F., R.S. and J.H.; formal analysis, P.B. (Péter Bencsik) and T.S.; investigation, P.B. (Péter Bencsik) and T.S.; data curation, P.B. (Péter Bencsik), T.S. and J.H.; writing—original draft preparation, J.H.; writing—review and editing, J.H., R.S., P.B. (Paulin Brosinsky) and P.F.; visualization, J.H. and R.S.; supervision, J.H.; project administration, J.H.; funding acquisition, R.S. and P.F. All authors have read and agreed to the published version of the manuscript.

Funding: This work was funded by Deutsche Forschungsgemeinschaft (DFG, German Research Foundation) (Project number 268555672—SFB 1213, Project B05). The project was supported by the Hungarian National Scientific Research Fund (OTKA-138223) of the National Research, Development and Innovation Office. P.B. (Péter Bencsik) was supported by the János Bolyai Research Scholarships of the Hungarian Academy of Sciences and by the New National Excellence Program of the Ministry of Human Capacities (ÚNKP-22-5-SZTE-542). T.S. was supported by the Cooperative Doctoral Programme for Doctoral Scholarships (KDP-2020) of the National Research, Development and Innovation Office. Project no. RRF-2.3.1-21-2022-00003 has been implemented with the support provided by the European Union. Project no. 2020-1.1.5-GYORSÍTÓSÁV-2021-00011 has been implemented with the support provided by the Ministry of Culture and Innovation of Hungary from the National Research, Development and Innovation Fund, financed under the 2020-1.1.5-GYORSÍTÓSÁV funding scheme.

Institutional Review Board Statement: All animal experiments were approved by the animal care and use committee of the Justus-414 Liebig University of Giessen, Germany, and were in accordance with the NIH Guide for the Care 415 and Use of Laboratory Animals (NIH Publication). The study was registered in Hungary under the number XXVIII./171/2018.

Data Availability Statement: The data presented in this study are available on request from the corresponding author.

Acknowledgments: The authors thank the following individuals: Anna Reis and Birgit Störr for their excellent technical assistance and Patricia Ewald and Christina Zartner for animal care.

Conflicts of Interest: P.F. is the founder and CEO of Pharmahungary Group, a group of R&D companies. The other authors declare no conflict of interest.

References

1. Di Lisa, F.; Kaludercic, N.; Carpi, A.; Menabò, R.; Giorgio, M. Mitochondrial pathways for ROS formation and myocardial injury: The relevance of $p66^{Shc}$ and monoamine oxidase. *Basic Res. Cardiol.* **2009**, *104*, 131–139. [CrossRef]
2. Zhou, B.P.; Lewis, D.A.; Kwan, S.-W.; Abell, C.W. Flavinylation of Monoamine Oxidase B. *J. Biol. Chem.* **1995**, *270*, 23653–23660. [CrossRef] [PubMed]
3. Murphy, M.P. How mitochondria produce reactive oxygen species. *Biochem. J.* **2009**, *417*, 1–13. [CrossRef] [PubMed]
4. Edmondson, D.E.; Binda, C.; Mattevi, A. Structural insights into the mechanism of amine oxidation by monoamine oxidases A and B. *Arch. Biochem. Biophys.* **2007**, *464*, 269–276. [CrossRef] [PubMed]
5. Youdim, M.B.; Bakhle, Y.S. Monoamine oxidase: Isoforms and inhibitors in Parkinson's disease and depressive illness. *Br. J. Pharmacol.* **2006**, *147* (Suppl. 1), S287–S296. [CrossRef]
6. Kirksey, T.J.; Kwan, S.W.; Abell, C.W. Arginine-42 and Threonine-45 are required for FAD incorporation and catalytic activity in human monoamine oxidase B. *Biochemistry* **1998**, *37*, 12360–12366. [CrossRef]
7. Binda, C.; Mattevi, A.; Edmondson, D.E. Structure-Function Relationships in Flavoenzyme-dependent Amine Oxidations. *J. Biol. Chem.* **2002**, *277*, 23973–23976. [CrossRef]
8. van Rhijn, J.-R.; Shi, Y.; Bormann, M.; Mossink, B.; Frega, M.; Recaioglu, H.; Hakobjan, M.; Gunnewiek, T.K.; Schoenmaker, C.; Palmer, E.; et al. Brunner syndrome associated MAOA mutations result in NMDAR hyperfunction and increased network activity in human dopaminergic neurons. *Neurobiol. Dis.* **2022**, *163*, 105587. [CrossRef]
9. Schömig, A.; Richardt, G. Cardiac Sympathetic Activity in Myocardial Ischemia: Release and Effects of Noradrenaline. *Basic Res. Cradiol.* **1990**, *85*, 9–30. [CrossRef]
10. Schömig, A.; Richardt, G.; Kurz, T. Sympatho-adrenergic activation of the ischemic myocardium and its arrhythmogenic impact. *Herz* **1995**, *20*, 169–186.
11. Rodríguez, M.J.; Saura, J.; Billett, E.E.; Finch, C.C.; Mahy, N. Cellular localization of monoamine oxidase A and B in human tissues outside of the central nervous system. *Cell Tissue Res.* **2001**, *304*, 215–220. [CrossRef] [PubMed]
12. Saura, J.; Nadal, E.; Berg, B.V.D.; Vila, M.; Bombi, J.; Mahy, N. Localization of monoamine oxidases in human peripheral tissues. *Life Sci.* **1996**, *59*, 1341–1349. [CrossRef] [PubMed]

13. Grimsby, J.; Toth, M.; Chen, K.; Kumazawa, T.; Klaidman, L.; Adams, J.D.; Karoum, F.; Gal, J.; Shih, J.C. Increased stress response and beta-phenylethylamine in MAOB-deficient mice. *Nat. Genet.* **1997**, *17*, 206–210. [CrossRef] [PubMed]
14. Maggiorani, D.; Manzella, N.; Edmondson, D.E.; Mattevi, A.; Parini, A.; Binda, C.; Mialet-Perez, J. Monoamine Oxidases, Oxidative Stress, and Altered Mitochondrial Dynamics in Cardiac Ageing. *Oxidative Med. Cell. Longev.* **2017**, *2017*, 1–8. [CrossRef] [PubMed]
15. Heusch, G. Cardioprotection: Chances and challenges of its translation to the clinic. *Lancet* **2013**, *381*, 166–175. [CrossRef]
16. Ferdinandy, P.; Andreadou, I.; Baxter, G.F.; Bøtker, H.E.; Davidson, S.M.; Dobrev, D.; Gersh, B.J.; Heusch, G.; Lecour, S.; Ruiz-Meana, M.; et al. Interaction of Cardiovascular Nonmodifiable Risk Factors, Comorbidities and Comedications With Ischemia/Reperfusion Injury and Cardioprotection by Pharmacological Treatments and Ischemic Conditioning. *Pharmacol. Rev.* **2023**, *75*, 159–216. [CrossRef]
17. Andreadou, I.; Schulz, R.; Papapetropoulos, A.; Turan, B.; Ytrehus, K.; Ferdinandy, P.; Daiber, A.; Di Lisa, F. The role of mitochondrial reactive oxygen species, NO and H2S in ischemia/reperfusion injury and cardioprotection. *J. Cell. Mol. Med.* **2020**, *24*, 6510–6522. [CrossRef]
18. Kaludercic, N.; Carpi, A.; Menabò, R.; Di Lisa, F.; Paolocci, N. Monoamine oxidases (MAO) in the pathogenesis of heart failure and ischemia/reperfusion injury. *Biochim. Biophys. Acta* **2011**, *1813*, 1323–1332. [CrossRef]
19. Du, C.-K.; Zhan, D.-Y.; Akiyama, T.; Inagaki, T.; Shishido, T.; Shirai, M.; Pearson, J.T. Myocardial interstitial levels of serotonin and its major metabolite 5-hydroxyindole acetic acid during ischemia-reperfusion. *Am. J. Physiol.-Heart Circ. Physiol.* **2017**, *312*, H60–H67. [CrossRef]
20. He, G.-H.; Hu, J.; Li, T.; Ma, X.; Meng, J.; Jia, M.; Lu, J.; Ohtsu, H.; Chen, Z.; Luo, X. Arrhythmogenic Effect of Sympathetic Histamine in Mouse Hearts Subjected to Acute Ischemia. *Mol. Med.* **2012**, *18*, 1–9. [CrossRef]
21. Genovese, A.; Spadaro, G. Highlights in cardiovascular effects of histamine and H1-receptor antagonists. *Allergy* **1997**, *52*, 67–78. [CrossRef] [PubMed]
22. He, Z.; Ma, C.; Yu, T.; Song, J.; Leng, J.; Gu, X.; Li, J. Activation mechanisms and multifaceted effects of mast cells in ischemia reperfusion injury. *Exp. Cell Res.* **2019**, *376*, 227–235. [CrossRef]
23. Valen, G.; Kaszaki, J.; Szabo, I.; Nagy, S.; Vaage, J. Histamine release and its effects in ischaemia-reperfusion injury of the isolated rat heart. *Acta Physiol. Scand.* **1994**, *150*, 413–424. [CrossRef]
24. Costiniti, V.; Spera, I.; Menabò, R.; Palmieri, E.M.; Menga, A.; Scarcia, P.; Porcelli, V.; Gissi, R.; Castegna, A.; Canton, M. Monoamine oxidase-dependent histamine catabolism accounts for post-ischemic cardiac redox imbalance and injury. *Biochim. Biophys. Acta* **2018**, *1864*, 3050–3059. [CrossRef]
25. Kaludercic, N.; Mialet-Perez, J.; Paolocci, N.; Parini, A.; Di Lisa, F. Monoamine oxidases as sources of oxidants in the heart. *J. Mol. Cell. Cardiol.* **2014**, *73*, 34–42. [CrossRef]
26. Yeung, A.W.K.; Georgieva, M.G.; Atanasov, A.G.; Tzvetkov, N.T. Monoamine Oxidases (MAOs) as Privileged Molecular Targets in Neuroscience: Research Literature Analysis. *Front. Mol. Neurosci.* **2019**, *12*, 143. [CrossRef] [PubMed]
27. Finberg, J.; Youdim, M.B. Modification of blood pressure and nictitating membrane response to sympathetic amines by selective monoamine oxidase inhibitors, types A and B, in the cat. *Br. J. Pharmacol.* **1985**, *85*, 541–546. [CrossRef] [PubMed]
28. Scotton, W.J.; Hill, L.J.; Williams, A.C.; Barnes, N.M. Serotonin Syndrome: Pathophysiology, Clinical Features, Management, and Potential Future Directions. *Int. J. Tryptophan Res.* **2019**, *12*, 1178646919873925. [CrossRef] [PubMed]
29. Antonucci, S.; Di Sante, M.; Tonolo, F.; Pontarollo, L.; Scalcon, V.; Alanova, P.; Menabò, R.; Carpi, A.; Bindoli, A.; Rigobello, M.P.; et al. The Determining Role of Mitochondrial Reactive Oxygen Species Generation and Monoamine Oxidase Activity in Doxorubicin-Induced Cardiotoxicity. *Antioxid. Redox Signal.* **2021**, *34*, 531–550. [CrossRef]
30. Cases, O.; Seif, I.; Grimsby, J.; Gaspar, P.; Chen, K.; Pournin, S.; Müller, U.; Aguet, M.; Babinet, C.; Shih, J.C.; et al. Aggressive Behavior and Altered Amounts of Brain Serotonin and Norepinephrine in Mice Lacking MAOA. *Science* **1995**, *268*, 1763–1766. [CrossRef]
31. Chen, K.; Holschneider, D.P.; Wu, W.; Rebrin, I.; Shih, J.C. A Spontaneous Point Mutation Produces Monoamine Oxidase A/B Knock-out Mice with Greatly Elevated Monoamines and Anxiety-like Behavior. *J. Biol. Chem.* **2004**, *279*, 39645–39652. [CrossRef] [PubMed]
32. Heger, J.; Hirschhäuser, C.; Bornbaum, J.; Sydykov, A.; Dempfle, A.; Schneider, A.; Braun, T.; Schlüter, K.D.; Schulz, R. Cardiomyocytes-specific deletion of monoamine oxidase B reduces irreversible myocardial ischemia/reperfusion injury. *Free Radic. Biol. Med.* **2021**, *165*, 14–23. [CrossRef] [PubMed]
33. Murphy, E.; Steenbergen, C. Gender-based differences in mechanisms of protection in myocardial ischemia–reperfusion injury. *Cardiovasc. Res.* **2007**, *75*, 478–486. [CrossRef]
34. Ostadal, B.; Ostadal, P. Sex-based differences in cardiac ischaemic injury and protection: Therapeutic implications. *Br. J. Pharmacol.* **2014**, *171*, 541–554. [CrossRef] [PubMed]
35. Ruiz-Meana, M.; Boengler, K.; Garcia-Dorado, D.; Hausenloy, D.J.; Kaambre, T.; Kararigas, G.; Perrino, C.; Schulz, R.; Ytrehus, K. Ageing, sex, and cardioprotection. *Br. J. Pharmacol.* **2020**, *177*, 5270–5286. [CrossRef]

36. Perrino, C.; Ferdinandy, P.; Bøtker, H.E.; Brundel, B.J.J.M.; Collins, P.; Davidson, S.M.; Ruijter, H.M.D.; Engel, F.B.; Gerdts, E.; Girao, H.; et al. Improving translational research in sex-specific effects of comorbidities and risk factors in ischaemic heart disease and cardioprotection: Position paper and recommendations of the ESC Working Group on Cellular Biology of the Heart. *Cardiovasc. Res.* **2020**, *117*, 367–385. [CrossRef]
37. Lagranha, C.J.; Deschamps, A.; Aponte, A.; Steenbergen, C.; Murphy, E. Sex Differences in the Phosphorylation of Mitochondrial Proteins Result in Reduced Production of Reactive Oxygen Species and Cardioprotection in Females. *Circ. Res.* **2010**, *106*, 1681–1691. [CrossRef]
38. Johnson, M.S.; Moore, R.L.; Brown, D.A. Sex differences in myocardial infarct size are abolished by sarcolemmal K_{ATP} channel blockade in rat. *Am. J. Physiol. Circ. Physiol.* **2006**, *290*, H2644–H2647. [CrossRef]
39. Robinson, D.S.; Davis, J.M.; Nies, A.; Ravaris, C.L.; Sylwester, D. Relation of Sex and Aging to Monoamine Oxidase Activity of Human Brain, Plasma, and Platelets. *Arch. Gen. Psychiatry* **1971**, *24*, 536–539. [CrossRef]
40. Zhang, Z.; Chen, K.; Shih, J.C.; Teng, C.T. Estrogen-Related Receptors-Stimulated Monoamine Oxidase B Promoter Activity Is Down-Regulated by Estrogen Receptors. *Mol. Endocrinol.* **2006**, *20*, 1547–1561. [CrossRef]
41. Sramek, J.J.; Murphy, M.F.; Cutler, N.R. Sex differences in the psychopharmacological treatment of depression. *Dialogues Clin. Neurosci.* **2016**, *18*, 447–457. [CrossRef] [PubMed]
42. Quitkin, F.M.; Stewart, J.W.; McGrath, P.J.; Taylor, B.P.; Tisminetzky, M.S.; Petkova, E.; Chen, Y.; Ma, G.; Klein, D.F. Are there differences between women's and men's antidepressant responses? *Am. J. Psychiatry* **2002**, *159*, 1848–1854. [CrossRef] [PubMed]
43. Curtis, M.J.; Hancox, J.C.; Farkas, A.; Wainwright, C.L.; Stables, C.L.; Saint, D.A.; Clements-Jewery, H.; Lambiase, P.D.; Billman, G.E.; Janse, M.J.; et al. The Lambeth Conventions (II): Guidelines for the study of animal and human ventricular and supraventricular arrhythmias. *Pharmacol. Ther.* **2013**, *139*, 213–248. [CrossRef]
44. Morkuniene, R.; Arandarcikaite, O.; Ivanoviene, L.; Borutaite, V. Estradiol-induced protection against ischemia-induced heart mitochondrial damage and caspase activation is mediated by protein kinase G. *Biochim. Biophys. Acta* **2010**, *1797*, 1012–1017. [CrossRef]
45. Pavón, N.; Martínez-Abundis, E.; Hernández, L.; Gallardo-Pérez, J.C.; Alvarez-Delgado, C.; Cerbón, M.; Pérez-Torres, I.; Aranda, A.; Chávez, E. Sexual hormones: Effects on cardiac and mitochondrial activity after ischemia-reperfusion in adult rats. Gender difference. *J. Steroid Biochem. Mol. Biol.* **2012**, *132*, 135–146. [CrossRef] [PubMed]
46. Hernández-Hernández, O.T.; Martínez-Mota, L.; Herrera-Pérez, J.J.; Jiménez-Rubio, G. Role of Estradiol in the Expression of Genes Involved in Serotonin Neurotransmission: Implications for Female Depression. *Curr. Neuropharmacol.* **2019**, *17*, 459–471. [CrossRef]
47. Querio, G.; Geddo, F.; Antoniotti, S.; Gallo, M.P.; Penna, C. Sex and Response to Cardioprotective Conditioning Maneuvers. *Front. Physiol.* **2021**, *12*, 667961. [CrossRef]
48. Nilsson, S.; Mäkelä, S.; Treuter, E.; Tujague, M.; Thomsen, J.; Andersson, G.; Enmark, E.; Pettersson, K.; Warner, M.; Gustafsson, J.A. Mechanisms of Estrogen Action. *Physiol. Rev.* **2001**, *81*, 1535–1565. [CrossRef]
49. Yang, S.H.; Liu, R.; Perez, E.J.; Wen, Y.; Stevens, S.M.; Valencia, T.; Brun-Zinkernagel, A.M.; Prokai, L.; Will, Y.; Dykens, J. Mitochondrial localization of estrogen receptor beta. *Proc. Natl. Acad. Sci. USA* **2004**, *101*, 4130–4135. [CrossRef]
50. Klaiber, E.L.; Broverman, D.M.; Haffajee, C.I.; Hochman, J.S.; Sacks, G.M.; Dalen, J.E. Serum estrogen levels in men with acute myocardial infarction. *Am. J. Med.* **1982**, *73*, 872–881. [CrossRef]
51. Purves-Tyson, T.D.; Handelsman, D.J.; Double, K.L.; Owens, S.J.; Bustamante, S.; Weickert, C.S. Testosterone regulation of sex steroid-related mRNAs and dopamine-related mRNAs in adolescent male rat substantia nigra. *BMC Neurosci.* **2012**, *13*, 95. [CrossRef]
52. Le, T.Y.L.; Ashton, A.W.; Mardini, M.; Stanton, P.G.; Funder, J.W.; Handelsman, D.J.; Mihailidou, A.S. Role of Androgens in Sex Differences in Cardiac Damage During Myocardial Infarction. *Endocrinology* **2014**, *155*, 568–575. [CrossRef]
53. Alnouti, Y.; Klaassen, C.D. Tissue Distribution, Ontogeny, and Regulation of Aldehyde Dehydrogenase (Aldh) Enzymes mRNA by Prototypical Microsomal Enzyme Inducers in Mice. *Toxicol. Sci.* **2008**, *101*, 51–64. [CrossRef]
54. Chen, C.-H.; Budas, G.R.; Churchill, E.N.; Disatnik, M.-H.; Hurley, T.D.; Mochly-Rosen, D. Activation of Aldehyde Dehydrogenase-2 Reduces Ischemic Damage to the Heart. *Science* **2008**, *321*, 1493–1495. [CrossRef] [PubMed]
55. Eaton, P.; Li, J.-M.; Hearse, D.J.; Shattock, M.J. Formation of 4-hydroxy-2-nonenal-modified proteins in ischemic rat heart. *Am. J. Physiol.-Heart Circ. Physiol.* **1999**, *276 Pt 2*, H935–H943. [CrossRef]
56. Santin, Y.; Fazal, L.; Sainte-Marie, Y.; Sicard, P.; Maggiorani, D.; Tortosa, F.; Yücel, Y.Y.; Teyssedre, L.; Rouquette, J.; Marcellin, M.; et al. Mitochondrial 4-HNE derived from MAO-A promotes mitoCa2+ overload in chronic postischemic cardiac remodeling. *Cell Death Differ.* **2020**, *27*, 1907–1923. [CrossRef]
57. Kaludercic, N.; Carpi, A.; Nagayama, T.; Sivakumaran, V.; Zhu, G.; Lai, E.W.; Bedja, D.; De Mario, A.; Chen, K.; Gabrielson, K.L.; et al. Monoamine Oxidase B Prompts Mitochondrial and Cardiac Dysfunction in Pressure Overloaded Hearts. *Antioxid. Redox Signal.* **2014**, *20*, 267–280. [CrossRef]
58. Ma, H.; Guo, R.; Yu, L.; Zhang, Y.; Ren, J. Aldehyde dehydrogenase 2 (ALDH2) rescues myocardial ischaemia/reperfusion injury: Role of autophagy paradox and toxic aldehyde. *Eur. Heart J.* **2010**, *32*, 1025–1038. [CrossRef] [PubMed]
59. Wang, Y.; Zhao, M.; Shi, Q.; Xu, B.; Zhu, C.; Li, M.; Mir, V.; Bers, D.M.; Xiang, Y.K. Monoamine Oxidases Desensitize Intracellular β1AR Signaling in Heart Failure. *Circ. Res.* **2021**, *129*, 965–967. [CrossRef] [PubMed]

60. Hahnova, K.; Brabcova, I.; Neckar, J.; Weissova, R.; Svatonova, A.; Novakova, O.; Zurmanova, J.; Kalous, M.; Silhavy, J.; Pravenec, M.; et al. β-Adrenergic signaling, monoamine oxidase A and antioxidant defence in the myocardium of SHR and SHR-mtBN conplastic rat strains: The effect of chronic hypoxia. *J. Physiol. Sci.* **2018**, *68*, 441–454. [CrossRef]
61. Csonka, C.; Kupai, K.; Kocsis, G.F.; Novák, G.; Fekete, V.; Bencsik, P.; Csont, T.; Ferdinandy, P. Measurement of myokardial infarct size in preclinical studies. *J. Pharmacol. Toxicol. Methods* **2010**, *61*, 163–170. [CrossRef] [PubMed]

Received: 22 December 2023 | Revised: 16 July 2024 | Accepted: 1 August 2024

DOI: 10.1111/bph.17345

Themed Issue: Non-coding RNA Therapeutics

THEMED ISSUE ARTICLE

Pharmacokinetics and cardioprotective efficacy of intravenous miR-125b* microRNA mimic in a mouse model of acute myocardial infarction

Tamara Szabados[1,2] | András Makkos[2,3] | Bence Ágg[2,3,4] | Bettina Benczik[2,3,4] | Gábor G. Brenner[3] | Márta Szabó[3] | Barnabás Váradi[3,4] | Imre Vörös[3] | Kamilla Gömöri[1,2] | Zoltán V. Varga[3] | Anikó Görbe[1,2,3] | Péter Bencsik[1,2] | Péter Ferdinandy[2,3]

[1]Cardiovascular Research Group, Department of Pharmacology and Pharmacotherapy, Albert Szent-Györgyi Medical School, University of Szeged, Szeged, Hungary

[2]Pharmahungary Group, Szeged, Hungary

[3]Cardiometabolic and HUN-REN-SU and MTA-SE System Pharmacology Research Group, Department of Pharmacology and Pharmacotherapy, and Center for Pharmacology and Drug Research & Development, Semmelweis University, Budapest, Hungary

[4]Center for Pharmacology and Drug Research & Development, Semmelweis University, Budapest, Hungary

Correspondence
Péter Ferdinandy, Cardiometabolic and MTA-SE System Pharmacology Research Group, Department of Pharmacology and Pharmacotherapy, Semmelweis University, Nagyvárad tér 4, H-1089, Budapest, Hungary.
Email: peter.ferdinandy@pharmahungary.com
Péter Bencsik, Cardiovascular Research Group, Department of Pharmacology and Pharmacotherapy, Albert Szent-Györgyi Medical School, University of Szeged, Dóm tér 12, H-6720, Szeged, Hungary.
Email: peter.bencsik@pharmahungary.com

Abstract

Background and purpose: MicroRNA (miRNA) therapy is a promising approach to induce cardioprotection. We have previously identified cardiac microRNA-125b* (microRNA-125b-2-3p; miR-125b*) as a potential cardioprotective miRNA, termed ProtectomiR. We aimed to characterize the pharmacokinetics and pharmacodynamics, and the effect of miR-125b* mimic on infarct size using an in vivo mouse model.

Experimental approach: To characterize the pharmacokinetics properties of miR-125b* mimic, a single injection of 10-μg miR-125b* mimic or its scramble miRNA control, or vehicle i.v. was given to C57BL/6 mice. MiR-125b* expression was measured from plasma, heart, kidney and liver samples. Effect of miR-125b* on area at risk and infarct size was assessed after 45-min coronary occlusion, followed by 24-h reperfusion; 10-μg miR-125b* mimic or 10-μg non-targeting miRNA mimic control or vehicle were administered via the right jugular vein at 10th mins of coronary occlusion. To assess molecular mechanism involved in cardioprotection, expression of mRNA targets of miR-125b* were measured from ventricular myocardium at 1, 2, 4, 8 or 24 h post-treatment using quantitative real time polymerase chain reaction.

Key results: MiR-125b* expression was markedly increased in plasma and myocardium 1 h, and in the liver 2h after treatment. Infarct size was significantly reduced after miR-125b* mimic treatment when compared to the vehicle. The expression of *Ccna2*, *Eef2k* and *Cacnb2* target mRNAs was significantly reduced 8 h after injection of miR-125b* mimic.

Abbreviations: Cacnb2, calcium channel, voltage-dependent, beta 2 subunit; Ccna2, cyclin 2A; cel-miR, microRNA derived from *Caenorhabditis elegans*; cDNA, complementary DNA; Dab2, disabled 2, mitogen responsive phosphoprotein; dsDNA, double stranded DNA; GO, gene ontology; LAD, anterior descending branch of the left coronary artery; miRNA or miR-NN, microRNA-NN; OT, off-target analysis; PoC, proof-of-concept; qRT-PCR, quantitative real time polymerase chain reaction; TTC, 2,3,5-triphenyl tetrazolium chloride.

Tamara Szabados, András Makkos, Péter Bencsik and Péter Ferdinandy contributed equally to this work.

Funding information
Ministry for Innovation and Technology in Hungary, Grant/Award Numbers: 2020-4.1.1.-TKP2020, 2020-1.1.5-GYORSÍTÓSÁV-2021-00011, TKP2021-EGA-23, TKP/ITM/NKFIH; European Union, Grant/Award Number: RRF-2.3.1-21-2022-00003; National Research, Development and Innovation Office of Hungary, Grant/Award Numbers: NVKP-16-1-2016-0017, VEKOP-2.3.2-16-2016-00002, VEKOP-2.3.3-15-2017-00016, OTKA-138223; Ministry for Innovation and Technology, Grant/Award Number: KDP-2020; New National Excellence Program of the Ministry for Innovation and Technology, Grant/Award Number: ÚNKP-23-4-II-SE-34; János Bolyai Research Scholarships of the Hungarian Academy of Sciences, Grant/Award Number: bo_481_21; New National Excellence Program of the Ministry of Human Capacities, Grant/Award Number: ÚNKP-23-5-SZTE-704; Albert Szent-Györgyi Medical School of the University of Szeged, Grant/Award Number: SZGYA2021

Conclusion and implications: This is the first demonstration of pharmacokinetic and molecular pharmacodynamic properties as well as the cardioprotective effect of miR-125b* mimic *in vivo*.

LINKED ARTICLES: This article is part of a themed issue Non-coding RNA Therapeutics. To view the other articles in this section visit http://onlinelibrary.wiley.com/doi/10.1111/bph.v182.2/issuetoc

KEYWORDS
infarct size; microRNA; miR-125b*; miR-125b-2-3p, non-coding RNA; off-target

1 | INTRODUCTION

1.1 | Cardioprotection

Myocardial ischemia–reperfusion injury (IRI) and its pathological consequences are the leading cause of death worldwide. However, cardioprotective therapeutics are still not available on the market, probably due to the complexity of the ischemic heart diseases (Ferdinandy et al., 2014; Ferdinandy et al., 2023). In preclinical studies, an abundant number of small molecules were proven to decrease infarct size, however none of them could be translated to human therapy. Therefore, to trigger effective cardioprotection, novel and multiple targets are needed (Davidson et al., 2019). For this purpose, microRNAs (miRNAs) provide a perfect opportunity because they can simultaneously affect several gene targets and are already introduced in the treatment of various pathologies including cardiovascular diseases (De Majo & De Windt, 2018; Makkos et al., 2021).

1.2 | MiRNA therapy

MiRNAs are short, approximately 18–25 nucleotide-long non-coding RNA sequences that are already available as advanced therapy medicinal products on the market. MiRNAs negatively regulate gene expression at the post-transcriptional level either by inhibition of the translation or promotion of the target mRNA degradation (Roberts et al., 2020). Entire cellular pathways can be regulated by a single miRNA (Uhlmann et al., 2012) and due to their pleiotropic nature, they gain great potential to become multi-target drugs for diseases with multifactorial origin (Hanna et al., 2019).

What is already known

- The protectomiR miR-125b* mimic was discovered in infarcted heart with ischemic conditionings
- miR-125b* mimic showed cardiocytoprotection in simulated ischemia/reperfusion injury in adult cardiac myocytes *in vitro*.

What does this study add

- The first demonstration of the pharmacokinetics of intravenous miR-125b* mimic
- miR-125b* mimic has a cardioprotective effect *in vivo* via a mechanism targeting several cellular pathways.

What is the clinical significance

- MiR-125b* mimic is a potential cardioprotective RNA therapeutic.

Two distinct approaches of the miRNA therapies are *miRNA mimics* and *antagomiRs*. *MiRNA mimics* are double-stranded sequences, including 'guide' strand, having the same sequence as its endogenous counterpart, and a not fully complementary passenger strand, which is degraded after the detachment (Krützfeldt et al., 2005; Winkle et al., 2021).

1.3 | miR-125b*

In a previous study, we have analysed the changes of miRNA expression in an *ex vivo* model of isolated rat hearts subjected to 30-min coronary occlusion followed by 120-min reperfusion and found several miRNAs with altered expression after ischemic pre- and/or postconditioning as compared with control ischemia–reperfusion injury (Varga et al., 2014). Out of the miRNAs showing altered expression, miRNA-125b* (miR-125b*) showed a pronounced down-regulation after ischemia–reperfusion injury as compared with non-ischemic control. Furthermore, miR-125b* was found to be counter-regulated by ischemic pre- or postconditioning as it showed a highly significant up-regulation as compared to ischemia–reperfusion injury. Therefore, the cardio-cytoprotective effect of miR-125b* was further validated in isolated neonatal cardiac myocytes subjected to simulated ischemia–reperfusion injury by using a miRNA mimic (Varga et al., 2014) and there was found a significantly increased cell viability in miR-125b* mimic-treated cells as compared with control ischemic cells.

The miR-125 family is a highly conserved mammalian miRNA family. MiR-125b* is the partially complementary, passenger strand of the matured miR-125b (miR-125b-2-3p) (Varga et al., 2018). It is expressed in various human and mouse tissues (for details, see Table S1).

In order to extrapolate the findings from cell culture experiments to *in vivo* animal models, it is necessary to set up an effective and suitable *in vivo* administration protocol for miR-125b*. However, there is no available data on the pharmacokinetic characteristics as well as on the impact on infarct size of exogenous miR-125b* mimic treatment against acute myocardial infarction (AMI).

Therefore, here we aimed to investigate the pharmacokinetic properties of miR-125b* mimic in blood as well as in several tissue samples and its pharmacodynamics by decreasing infarct size as administered intravenously in an *in vivo* mouse model of acute myocardial infarction (AMI).

2 | METHODS

2.1 | Study design

The animal experiments were designed as recommended in the ARRIVE 2.0 guidelines (Percie du Sert et al., 2020) supplemented by the proposed reporting data in our recently published meta-analysis (Sayour et al., 2023), by which we aimed to improve the rigour and transparency of scientific research. To highlight the quality control of the present study, we performed all the experiments in a blinded and randomized manner (Sayour et al., 2023).

As an initial step, we performed an explorative pharmacokinetics to investigate the biodistribution of miR-125b* mimic and to measure gene expression of selected mRNA targets, respectively. On the basis of these data, we determined the time of administration of miR-125b* mimic and the follow-up time of animals to measure infarct size. Then, we performed a pilot proof-of-concept (PoC-1) study in a mouse acute myocardial infarction model, where miR-125b* mimic was administered at the 10th min of 45-min test ischemia, and we measured infarct size 24 h after the release of coronary occlusion and used a scrambled miRNA sequence as a control. We obtained a slight cardioprotection in both miR-125b* mimic and the scramble miRNA without reaching the statistically significant level. Therefore, we performed further analyses (gene ontology [GO] and off-target analysis [OT]) to improve the study design in further miRNA studies. Based on the results of GO and OT analyses, a second proof-of-concept study was conducted by using a different control miRNA sequence, *Caenorhabditis elegans* microRNA-239b (cel-miR-239b) mimic (see also in Figure 1). Finally, we investigated the potential underlying mechanism of the cardioprotective effect of miR-125b* mimic by using molecular pharmacodynamics.

2.2 | Animals

This investigation was carried out according to the Guide for the Care and Use of Laboratory Animals published by the US National Institutes of Health (NIH publication No. 85-23, revised 1996) and to the EU Directive (2010/63/EU) and with the permission of the National Scientific Ethical Committee on Animal Experimentation (approval ID: XXVIII./171/2018) and permitted by the government (National Food Chain Safety Office and Animal Health Directorate of the Government Office for Pest County (PE/EA/1784-7/2017). Further, animal studies are also reported in compliance with the ARRIVE guidelines (Percie du Sert et al., 2020) and with the recommendations made by the *British Journal of Pharmacology* (Lilley et al., 2020).

All animal experiments were conducted on 10- to 14-week-old male C57BL/6 mice (RRID:MGI:2159769) obtained from Charles River Laboratories. In the pharmacokinetic study, mice weight was 21.3 ± 0.27 g; in the ischemia/reperfusion studies, mice weighed 26.4 ± 0.2 g in PoC1 and 27.7 ± 0.17 g in PoC2 (Table S2). All mice were housed in individually ventilated cages (Sealsafe IVC system, Tecniplast S.p.a., Varese, Italy), which conforms to the size recommendations of the 2010/63/EU Directive. Animals were kept in a 12 h light/12 h dark cycle in a room with a controlled temperature (22 ± 2°C). They had free access to standard rodent chow (SAFE A40, Innovo Ltd., Isaszeg, Hungary) and filtered tap water all time, without fasting before the experiments. The animals were acclimatized in the housing facility for at least 5 days prior to the start of the animal experiments.

2.3 | MicroRNA preparations

Dharmacon rno-miR-125b-2-3p miRIDIAN mimic (CTM-686138) referred as miR-125b* mimic, Dharmacon scr- miRIDIAN control (CTM-487903) referred as scramble miRNA or Dharmacon cel-miR-239b Control (CTM-686137) referred as non-targeting control cel-

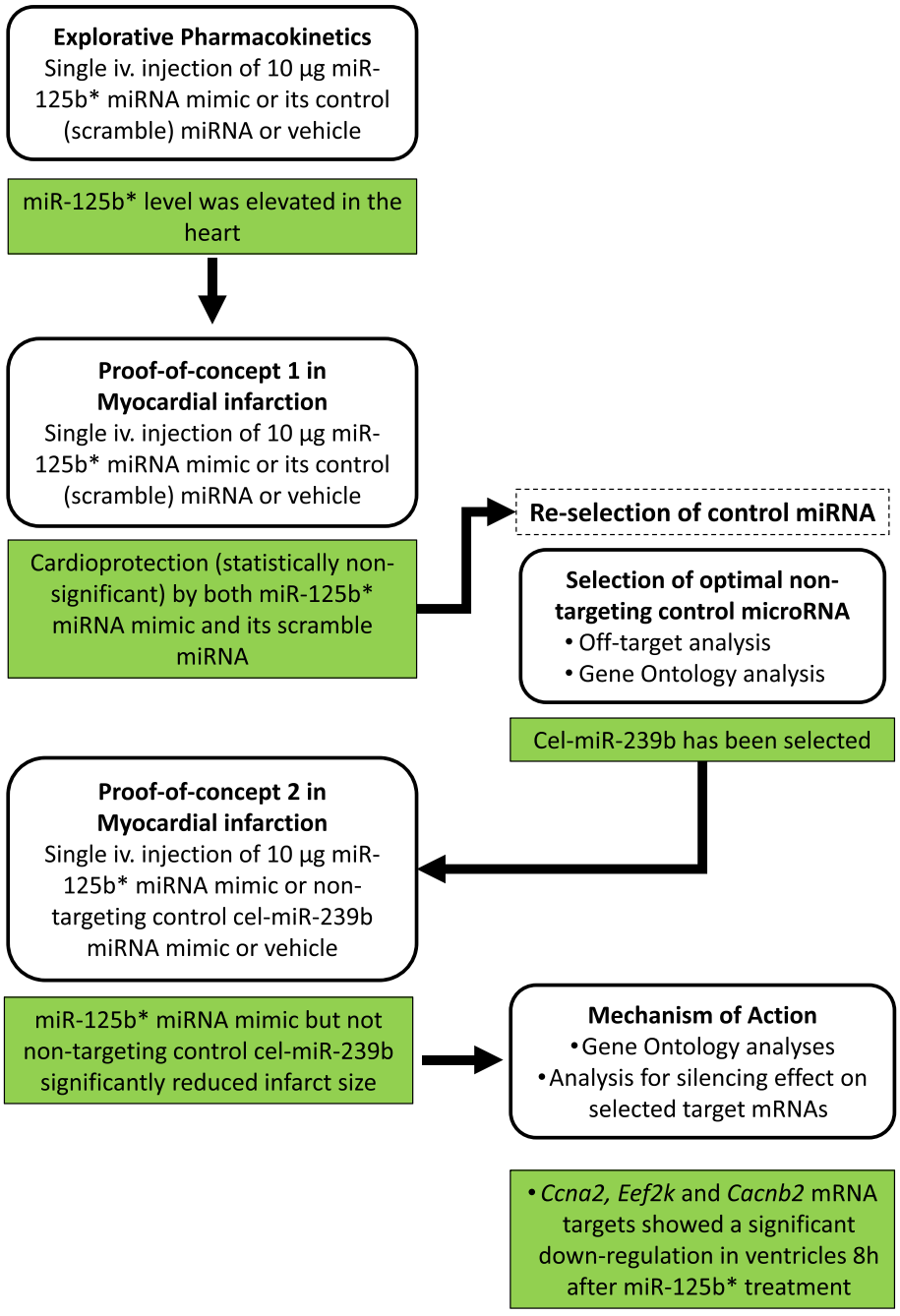

FIGURE 1 Study design and major results. *Ccna2*: Cyclin 2A; *Eef2k*: Eukaryotic elongation factor-2 kinase; *Cacnb2*: Calcium voltage-gated channel auxiliary subunit beta 2.

miR-239b mimic was purchased from Dharmacon/Horizon Discovery (Cambridge, United Kingdom); sequence of the guide and passenger strands are available in Table S3.

Desalted miRNA mimics were diluted in RNase-free water to prepare 20-μM stock solution and stored at −20°C. On the day of the experiment, the stock solutions were further diluted by the addition of RNase-free 10× PBS and added to MaxSuppresor In Vivo RNA-LANCEr II neutral lipid emulsion (Bioo Scientific, Cat. No. 3410-01) based on the manufacturer instructions. After ultrasonic sonication for 2 min, 10 μg of miRNA mimics were prepared in a final volume of 300 μl by aspirating into a syringe for injection.

2.4 | Explorative pharmacokinetics and molecular pharmacodynamics

To measure the pharmacokinetic properties, a vehicle group, a scramble miRNA and a miR-125b* mimic treatment group were applied. In the vehicle group, RNase-free water was substituted for the stock solution of miRNA mimics to complete the addition of PBS and neutral lipid emulsion. In the scramble miRNA and in the miR-125b* mimic treatment groups, 10 μg miRNA was used per mouse. All treatments were administered intravenously through the tail vein. A single dose of 10 μg of miR-125b* was selected based on data of a previous paper showing effective cardioprotection after coronary ligation in

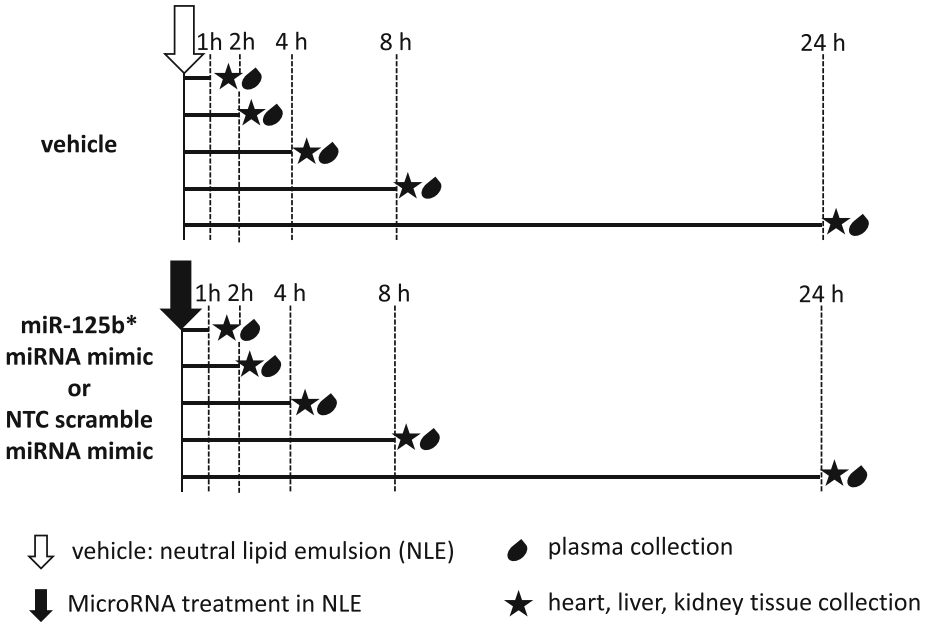

FIGURE 2 Experimental protocol for pharmacokinetics.

C57Bl/6 mice by administration 10-µg miR-302-367 per mouse (of the same weight range) and using the same neutral lipid emulsion as vehicle (Tian et al., 2015) as in the present study.

2.5 | Experimental protocol for pharmacokinetics

Study protocol is demonstrated on Figure 2. Mice were placed in restraint devices and a heat lamp was used to heat their tails to approximately 37°C. The injection site was cleaned and disinfected, and 300-µl emulsion was injected into the tail vein at a slow rate (~20 µl·s^{-1}). Then pressure was briefly applied to the injection site. The animals were observed for the protocol time (1, 2, 4, 8 or 24 h) and then killed by a cervical dislocation following **pentobarbitone** anaesthesia. Immediately prior to giving pentobarbitone approximately 500-µl blood was collected from the retro-orbital sinus into tripotassium-ethylene diamine tetraacetic acid (K3-EDTA) tubes. Blood was then centrifuged at 2 × 2500 g at 4°C to obtain a cell-free plasma fraction. Cell-free plasma fraction was immediately frozen in liquid nitrogen and stored at −80°C. After termination, the chest was opened and the animals were perfused with warm physiological saline via the apex of the left ventricle. The saline was perfused through the animal's circulatory system under hydrostatic pressure. Perfusion was continued for 2–5 min until all visible organs had turned grey. The heart was then removed, the left ventricle isolated and immediately frozen in liquid nitrogen by cutting it into small pieces.

2.6 | Total RNA isolation

Total RNA was isolated from 25 mg of left ventricular myocardium, kidney and liver tissue samples using Direct Zol RNA MiniPrep (Zymo Research, Irvine, CA, USA; Cat. No. #R2050), according to the manufacturer instructions. DNase I (Thermo Fischer Scientific, Waltham, MA, USA; Cat. No. #EN0521) treatment was applied after total RNA elution in RNase-free water. Total RNA was isolated from plasma using the Qiagen miRNeasy Serum/Plasma kit (Qiagen, Hilden, Germany; Cat. No. #217184). RNA concentration was determined by spectrophotometry (NanoDrop, Thermo Fischer Scientific, Waltham, MA, USA).

2.7 | Measurement of miR-125b* expression

Complementary DNA (cDNA) was synthesized from 10-ng total RNA using the Qiagen miRCURY RT kit (Qiagen, Hilden, Germany; Cat. No. #339340) according to the manufacturer's instructions. cDNA was further diluted 60× with RNase-free water. quantitative real time polymerase chain reaction (qRT-PCR) reactions were performed on a LightCycler® 480 II instrument (Roche, Penzberg, Germany) by using a miRCURY PCR assay kit (Qiagen, Hilden, Germany; Cat. No. #339306). Polymerase was heat-activated for 2 min at 95°C, and targets were amplified and quantified in 45 cycles (denaturation: 10 s at 95°C; combined annealing/synthesis: 60 s at 56°C). Forward and reverse primers for miR-125b* (Qiagen, Hilden, Germany; Cat. No. YP00205315) were used. In the case of tissue samples U6 snRNA (Qiagen, Hilden, Germany; Cat. No. YP00203907), while in the case of plasma samples, miR-191 (Qiagen, Hilden, Germany; Cat. No. YP00205175) was used as a housekeeping gene. Results were calculated with the $2^{-\Delta\Delta Cp}$ evaluation method to measure the expression level of miR-125b*.

2.8 | Selection of miR-125b* target genes

To validate target engagement in the heart as a result of intravenous miR-125b* mimic treatment, five miR-125b* target genes were

selected. Target genes were selected via two methods:- (1) miRTarBase version 4.5 (Huang et al., 2022), a collection of previously published miRNA-target interactions, was used to identify two experimentally validated targets of miR-125b*, namely, *cyclin 2A (Ccna2)* and ***eukaryotic elongation factor-2 kinase (Eef2k)*** genes (Xu et al., 2016). (2) A combination of two *in silico* predicted miRNA-target interaction databases (miRDB version 5.0 (Wong & Wang, 2015) and TargetScan version 7.2 (McGeary et al., 2019) and an additional PubMed literature search was performed to identify additional possible targets of miR-125b*. A PubMed search was performed on 6 January 2021, with the search terms: gene_symbol AND (myocard* OR heart). This way *calcium channel, voltage-dependent, beta 2 subunit (Cacnb2)*, *lysine (K)-specific demethylase 6A (Kdma6)* and *disabled 2, mitogen responsive phosphoprotein (Dab2)* was selected. For further information, see Table S4.

2.9 | Measurement of miR-125b* target engagement by qRT-PCR

cDNA was synthesized from 1-μg total RNA using a Sensifast cDNA synthesis kit (Bioline, London, UK; Cat. No. #BIO-65053) according to the manufacturer protocol. cDNA was further diluted 20× with RNAse-free water. qRT-PCR reactions were performed on a LightCycler® 480 II instrument (Roche, Penzberg, Germany) by using the SensiFAST SYBR Green master mix (Bioline, London, UK; Cat No. #BIO-98005). Polymerase was heat-activated for 2 min at 95°C, and targets were amplified and quantified in 40 cycles (denaturation: 5 s at 93°C; annealing: 10 s at 60°C; synthesis: 20 s at 72°C). Forward and reverse primers for the *Ccna2*, *Eef2k*, *Cacnb2*, *Kdm6a* and *Dab2* genes were used for analysis. **Peptidylprolyl isomerase A (cyclophilin A; Ppia)** was used as a housekeeping gene. Sequences of primers are shown in Table S5. Results were calculated with the $2^{-\Delta\Delta Cp}$ evaluation method.

2.10 | *In vivo* acute myocardial infarction protocol

Ischemia–reperfusion injury (IRI) was induced *in vivo* by external occlusion of the anterior descending branch of the left coronary artery (LAD) as described before (Boengler et al., 2017; Heger et al., 2023). Briefly, mice were anaesthetised with pentobarbitone (90 mg·kg^{-1}, i.p.). For analgesia, **buprenorphine** (0.05 mg·kg^{-1}) was administered (multidose 0.3 mg·ml^{-1}) subcutaneously 10 min before the start of the surgery and at the end of the ischemia. Shortly after anaesthesia induction, when the animals did not respond to painful stimuli, the chests of mice were depilated and mice were intubated via the trachea and mechanically ventilated with room air (6.2 ml·kg^{-1}, 120–150 breath·min^{-1}) (Harvard Instruments, Minivent Type 845). Depth of anaesthesia was monitored by toe and tail pinching, and when needed, maintenance dose of pentobarbitone (45 mg·kg^{-1}, i.p.) was given. The body core temperature was maintained at 37 ± 1°C using a constant temperature heating pad. The right jugular vein was cannulated for the administration of pharmacological treatments as well as for the maintenance of fluid homeostasis with physiological saline. The chest was opened at the 4th intercostal space and the left artery descending (LAD) coronary was visualized. After the pericardium was removed, an 8-0 Prolene (Ethicon, Cincinnati, USA; Cat. No. W2777) suture was placed at the middle portion of the LAD. To ensure LAD occlusion (45 min) as well as its subsequent release (24 h), the string was looped and a small piece of a plastic cannula was placed onto the surface of the heart directly above the coronary artery before the loop was pulled tight. Heart rate, signs of myocardial infarction (e.g. ST-segment elevation and ventricular arrhythmias) and body core temperature were monitored throughout the experiment (Haemosys Software, MDE, Hungary). Mice were administered 10-μg miRNA125b* mimic or scrambled miRNA or cel-miR-239b mimic or vehicle (Neutral Lipid Emulsion) in a volume load of 300 μl. MiRNA was administered via intravenous slow bolus injection (~20 μl·s^{-1}) at the 10th min of coronary occlusion, to mimic clinical scenario with an early administration during emergency care until the start of recanalization therapy, while letting some time for haemodynamic stabilization after coronary occlusion. At the end of the 45-min ischemia, a 6-0 Prolene (Ethicon, Cincinnati, USA; Cat. No. 8610H) suture was used to sew the ribs and the skin of the mouse. The chest was closed in layers, the wound was treated with Braunol®, then the animals were put into their cages to recover.

2.11 | Infarct size measurement

Twenty-four hours after the ischemia, mice were re-anaesthetised with pentobarbitone (90 mg·kg^{-1}, i.p.), the chest was re-opened and the coronary artery was re-occluded, then 2% Evans-blue dye was injected through the inferior vena cava to delineate the area at risk. The heart was excised from the chest, and the atria and right ventricle were removed. Left ventricle was cut into 1-mm-thick slices. The area at risk (AAR) was defined as the size of the area not affected by Evans-blue dye.

Infarct size was determined by standard 2,3,5-triphenyl tetrazolium chloride (TTC) as previously described by Csaba Csonka (Csonka et al., 2010). TTC was dissolved in 0.1 M of phosphate buffer of pH 7.4 and slices were incubated in 1% TTC solution for 10 min. Slices were photographed between glass plates (Canon, SX60 HS). The evaluation was carried out with InfarctSize software (Infarctsize 2.5, Pharmahungary 2000 Ltd.) by two blinded experienced observers. The final result is not the average of the two evaluators but the consensus reached by comparing the evaluations by the experts. Animals were excluded from further evaluation either due to less than 10% of AAR, myocardial territory excluded from the circulation by LAD occlusion, or technical failure of Evans Blue staining.

2.12 | Experimental groups of PoC acute myocardial infarction study

Study protocol is demonstrated on Figures 3a and 6a. Two sets of experiment were performed. Mice were randomized into 3 groups in

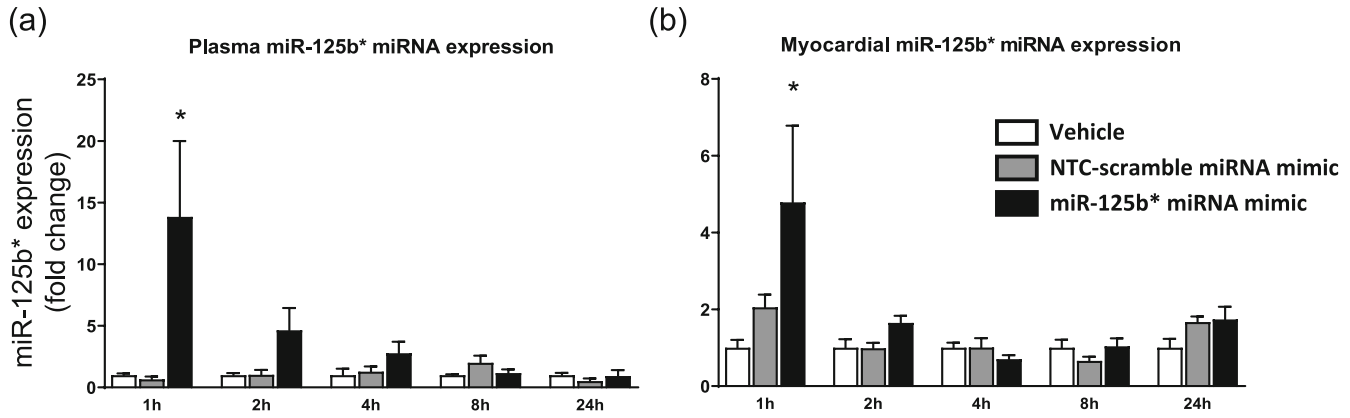

FIGURE 3 Results of pharmacokinetic study: miR-125b* expression measured after single 10 μg of miR-125b* mimic or scrambled miRNA or vehicle intravenous injection in the plasma (a) and in the myocardium (b); *marked increase without using any statistical analysis due to low sample size (n < 5) . For n numbers, see Table S6, panel A.

both PoC studies: (i) miR-125b* mimic-treated; (ii) control-miRNA (scramble or cel-miR-239b, see below) -treated; and (iii) vehicle-treated groups. In PoC-1, mouse scramble miRNA was used as control, whereas in PoC-2, *C. elegans* miR-239b (cel-miR-239b) mimic served as non-targeting control miRNA mimic, which was considered to be an appropriate alternative as similar endogenous sequence was not found by a single sequence search in miRBase database among the relevant species.

2.13 | MiRNA-like off-target prediction, target gene set similarity analysis and GO analysis

Scramble miRNA and non-targeting control cel-miR-239b mimic candidate sequences were subjected to miRNA-like off-target analysis to reveal possible non-desired effects. In this analysis, predicted regulation by guide, or passenger strand, or by both strands were considered. For seed complementarity and sequence feature-based miRNA-like off-target prediction Perl scripts of the TargetScan algorithm (Agarwal et al., 2015), along with three prime untranslated region (3′-UTR) and open reading frame sequence files were downloaded from TargetScan-Mouse version 7.2 website. Minor adjustments were applied to the Perl scripts to be able to run it with custom mouse data. Generated predictions include all possible target site hits regarding the downloaded 3′-UTR sequences and total context++ score was calculated for each transcript. After preprocessing, the predicted TargetScan results were used as input database with total context++ score threshold of −0.2 (Kimura et al., 2019) for miRNAtarget™ software (mirnatarget.com; Pharmahungary, Szeged, Hungary) to construct miRNA-target interaction networks for the scramble miRNA and cel-miR-239b mimic candidates and to calculate node strength values combined with total context++ scores. MiR-125b* mimic was also subjected to the same prediction workflow to be able to analyse its cardioprotective mechanism of action and to be able to perform target gene set similarity-based comparisons with the two different controls. Predicted miRNA-like off-targets for cel-miR-239b and for scramble sequences were compared with the target gene set of miR-125b* mimic.

GO enrichment analysis (Ashburner et al., 2000; Gene Ontology Consortium, 2021) was performed to reveal biological processes possibly affected by the scramble miRNA or by the non-targeting control cel-miR-239b mimic sequences or by the miR-125b* mimic sequence through their target genes. Over-representation analysis was implemented with the use of clusterProfiler R package (Yu et al., 2012) (version 3.18.0) using enricher function on biological process ontology and mouse annotations from GO release 2020-10-09 (Carbon & Mungall, 2018). Relation types of 'part_of' and 'is_a' were considered for the hierarchy. For the analysis, all mouse genes with GO annotation were used as background genes, and the values of minimal and maximal size of gene sets annotated for testing were set to 1 and to the size of the gene set size with GO annotation to include all possible enriched terms, respectively. Mechanism of action of miR-125b* and predicted regulatory effect differences between the sequences were highlighted by further analysing the enrichment results. Most specific GO terms without any significantly enriched child term of miR-125b* were identified as relative leaf terms. A term was considered as significantly enriched if its false discovery rate (FDR)-adjusted P value was ≤0.05. From relative leaf terms, the most relevant terms were selected with keywords:- heart, cardi*, vess*, aort*, arter*, ven* and visualized together for all three sequences.

2.14 | MIR-125B* tissue expression and distribution in human and mouse

Human miR-125b* expression data in various tissues were obtained from the TissueAtlas database (https://ccb-web.cs.uni-saarland.de/tissueatlas2/patterns/hsa/mirna/hsa-miR-125b-2-3p) and mouse miR-125b* expression data were obtained from the Tabula Muris and Tabula Muris Senis collections embedded in TissueAtlas website (https://ccb-web.cs.uni-saarland.de/tissueatlas2/patterns/mmu/mirna/

mmu-miR-125b-2-3p/). Human expression data in the database are derived from two female and four male donors (altogether 21 organs, 188 samples) who died of natural causes and a number of associated diseases (Keller et al., 2022), and mouse expression data are derived from 7 different organs of 37 healthy young adult mice (Tabula Muris, 2020; Tabula Muris et al., 2018). For detailed expression data, see Table S1.

2.15 | mRNA-omics and principal component analysis

Approximately 30 mg of left ventricular tissue powder sampled from the animals included in the pharmacokinetics study was placed in a 1.5-ml Eppendorf LoBind tube containing 4 glass beads (1.7- to 2.1-mm diameter, Carl Roth, Karlsruhe, Germany) and 150 µl of TRI Reagent (Zymo Research, Irvine, CA, USA). The Eppendorf tube was firmly attached to a SILAMAT S5 vibrator (Ivoclar Vivadent, Schaan, Liechtenstein) in order to disrupt and homogenize the tissue for 2x15s.

Total RNA was extracted using Direct-zol RNA MiniPrep System with on-column DNAse I treatment according to the manufacturer's (Zymo Research, Irvine, CA, USA) protocol. The RNA Integrity Numbers and RNA concentration were determined by RNA ScreenTape system with 2200 Tapestation (Agilent Technologies, Santa Clara, CA, USA) and RNA HS Assay Kit with Qubit 3.0 Fluorometer (Thermo Fisher Scientific, Waltham, MA, USA), respectively.

For Gene Expression Profiling (GEx) library construction, QuantSeq 3′mRNA-Seq Library Prep Kit FWD for Illumina (Lexogen GmbH, Wien, Austria) was applied according to the manufacturer's protocol. The quality and quantity of the library were determined by using High Sensitivity DNA1000 ScreenTape system with 2200 Tapestation (Agilent Technologies, Santa Clara, CA, USA) and dsDNA HS Assay Kit with Qubit 3.0 Fluorometer (Thermo Fisher Scientific, Waltham, MA, USA), respectively. Pooled libraries were diluted to 2 pM for 1 × 86 bp single-end sequencing with 75-cycle High Output v2.5 Kit on the NextSeq 500 Sequencing System (Illumina, San Diego, CA, USA) according to the manufacturer's protocol.

Adapter sequences, polyadenylate tails and bases with Phred score lower than 30 were trimmed, and reads with a length below 19nt were filtered out by Cutadapt (version 4.1) (Williams et al., 2016). Quality control measurements were performed by FastQC (version 0.11.9) and MultiQC (version 1.13) (Ewels et al., 2016). Gene expression profiles were assessed by Hisat2 (version 2.2.1) - Samtools (version 1.15.1) - featureCounts (version 2.0.1) - DESeq2 (version 1.34.0) bioinformatics workflow using Ensembl GRCm38 reference genome and annotation (Danecek et al., 2021; Kim et al., 2015; Li et al., 2009; Liao et al., 2014; Love et al., 2014). To visualize the relationships between whole gene expression profiles, principal component analysis was applied on normalized read counts transformed by regularized logarithm (Pearson, 1901). The entire bioinformatics analysis of RNA-sequencing was performed in Conda (version 4.12.0) environment with R version 4.1.3 (Conda Documentation, n.d.; R Core Team, 2018).

2.16 | Statistics

The data and statistical analysis comply with the recommendations on experimental design and analysis in pharmacology (Curtis et al., 2022). Statistical analyses were performed using GraphPad Prism version 9.2 (GraphPad Software, San Diego, CA, USA). Unless noted otherwise, all data are expressed as the mean ± SEM. In explorative pharmacokinetics and molecular pharmacodynamics (PD) studies, given that the sample size for certain groups is below n = 5 (ranging from 3 and 6; for detailed sample size data, see Supplementary Table S6) we did not apply any statistics (see Curtis et al., 2022). Samples sizes subjected to statistical analysis were at least 5 animal per group, where n = number of indepentent values. One-way analysis of variance (ANOVA) with Dunnett post hoc test was used to show statistically significant differences in area at risk and infarct size data in both PoC studies. Post hoc tests were conducted if ANOVA achieved $P < 0.05$. All-cause mortality and incidence of arrhythmias were analysed with Chi-square test. Differences were considered significant at values of $P < 0.05$.

2.17 | Materials

Pentobarbitone was purchased from Le Vet Pharma (Oudewater, The Netherlands), while tripotassium-ethylene diamine tetraacetic acid (K3-EDTA) tubes purchased from Sarstedt Ltd. (Lower Saxon; Germany; Cat. No. 20.1341.100). Liquid nitrogen was obtained from Messer Hungarogaz Ltd. (Szeged, Hungary) and buprenorphine from Richter Pharma AG (Wels, Austria), while Braunol® from Braun (Germany) and Evans-blue dye from Sigma-Aldrich (St. Louis, MO, USA; Cat. No. E2119). 2,3,5-triphenyl tetrazolium chloride (TTC) was purchased from (Merck Biosciences (Germany; Cat. No. 108380). Details of other materials and suppliers were provided in the specific sections.

2.18 | Nomenclature of targets and ligands

Key protein targets and ligands in this article are hyperlinked to corresponding entries in the IUPHAR/BPS Guide to PHARMACOLOGY http://www.guidetopharmacology.org and are permanently archived in the Concise Guide to PHARMACOLOGY 2023/24 (Alexander et al., 2023).

3 | RESULTS

3.1 | Explorative pharmacokinetics

To measure the pharmacokinetic properties of miR-125b* mimic, we determined the expression level of miR-125b* from plasma, myocardium, liver and kidney samples, 1, 2, 4, 8 or 24 h after the administration of 10 µg miR-125b*mimic as single intravenous bolus injection (for experimental protocol, see Figure 2).

3.1.1 | miR-125b* expression in blood plasma

miR-125b* level in the blood plasma showed a marked increase 1 h after tail vein injection of miR-125b* mimic. However, this increase was reduced at 2 and 4 h, while after at 8 and 24 h, miR-125b* level did not show any difference when compared with the time-matched vehicle group. Scramble miRNA did not alter miR-125b* expression at any time point (Figure 3, panel a).

3.1.2 | miR-125b* expression in the myocardium

Similarly for plasma miR-125b*, the level was markedly increased in the heart 1 h after its administration via the tail vein compared with that of the vehicle-treated group. At 2 h and the later time points, there was no significant difference between the groups. Scramble miRNA did not alter cardiac miR-125b* expression at any time point (Figure 3, panel b).

3.1.3 | miR-125b* expression in the liver and the kidney

To characterize tissue distribution features of miR-125b* mimic, the expression level of miR-125b* was detected in the liver and the kidney. In the liver, at 1 h after intravenous administration of miR-125b*, we did not observe any difference between groups; however, at 2 h, its expression was markedly increased as compared with the time-matched vehicle. At 4, 8 and 24 h, the difference between the groups was abolished. In the kidney, there was a marked increase in miR-125b* expression 1 h after its administration as compared with the time-matched vehicle. At 2 h, a sudden decline could be detected with no difference between groups. However, at 4, 8 and 24 h we observed a gradual increase both in the miR-125b* mimic- and in the scramble miRNA-treated groups compared with the time-matched vehicle group (Figure S1, panels A and B, respectively).

3.2 | Proof-of-concept studies for cardioprotection

3.2.1 | Effect of miR-125b* intravenous administration on infarct size (a pilot proof of concept study; PoC-1)

To assess the potential cardioprotective effect of miR-125b* mimic in a pilot proof-of-concept study (PoC-1), we administered it intravenously at the 10th min of coronary occlusion in a mouse acute myocardial infarction model. The infarct size was then assessed at the end of 45-min LAD occlusion followed by 24-h reperfusion using the widely accepted Evans blue/TTC staining method (for experimental protocol see Figure 4, panel a). An average of approximately 30% of the left ventricle was exposed to the ischemic insult (Figure 4, panel b). However, the left ventricle area at risk did not differ significantly among the groups. In PoC-1, treatment with miR-125b* mimic and scramble miRNA showed mild cardioprotection with a statistically non-significant reduction of infarct size (Figure 4, panel c).

3.2.2 | MiRNA-like off-target prediction, target gene set similarity analysis and GO analysis

Due to the surprising infarct size-decreasing trend of the scramble miRNA mimic, further analyses were performed to find a more optimal neutral miRNA sequence, which does not evoke cardioprotection even as a protective tendency. We carried out an off-target analysis combined with GO analysis of miR125b* and control miRNAs. *In silico* target similarity- and functionality-based results of miRNA-like off-target analysis suggested that the cel-miR-239b sequence is more suitable candidate for non-targeting control miRNA mimic than the control scramble miRNA sequence. By miRNA-like off-target analysis workflow, we identified 11,086, 7,778 and 10,739 potential gene s that could be regulated either by the scramble-miRNA, by cel-miR-239b or by miR-125b*, respectively. As for the requirements for a control sequence in general, the less overlapping targets the control has the higher the chance for being a suitable negative control. Thus, the target gene set size of the cel-miR-239b sequence compared with the scramble sequence suggests lower chance for undesired effects. The scramble sequence shares 7223 common predicted targets with miR-125b*, and this intersection in case of cel-miR-239b sequence contains only 5320 common predicted targets (see Figure 5). Based on the target prediction using both guide and passenger strands of scramble miRNA and miR-125b*, 67.25% of the predicted targets were overlapping (see Figure 5), which may explain the tendency for protective effect of scramble miRNA provided by the manufacturer of miR-125b* mimic (Dharmacon/Horizon Discovery, Cambridge, United Kingdom). However, it cannot be excluded that the scramble miRNA sequence regulates different pathways, which may also be responsible for cardioprotection. When comparing target gene set of miR-125b* to target gene set of either candidate control sequences (i.e. scramble and cel-miR-239b), larger intersection size in case of scramble sequence suggests higher similarity between the regulatory mechanisms of the two compared sequences. Which is in line with the functional analysis of the targets. Cardiovascular-related biological processes potentially affected by miR-125b* with highest relevance as revealed by GO enrichment analysis include atrioventricular canal development, cardiac pacemaker cell development, cardiac muscle cell proliferation, atrial cardiac muscle cell action potential and branching involved in blood vessel morphogenesis. For the complete list of processes, see Figure 6 and Table S10. When comparing the GO enrichment patterns of the selected relative leaf terms, the scramble sequence showed higher degree of similarity to the miR-125b* than that of the cel-miR-239b (see Figure 6).

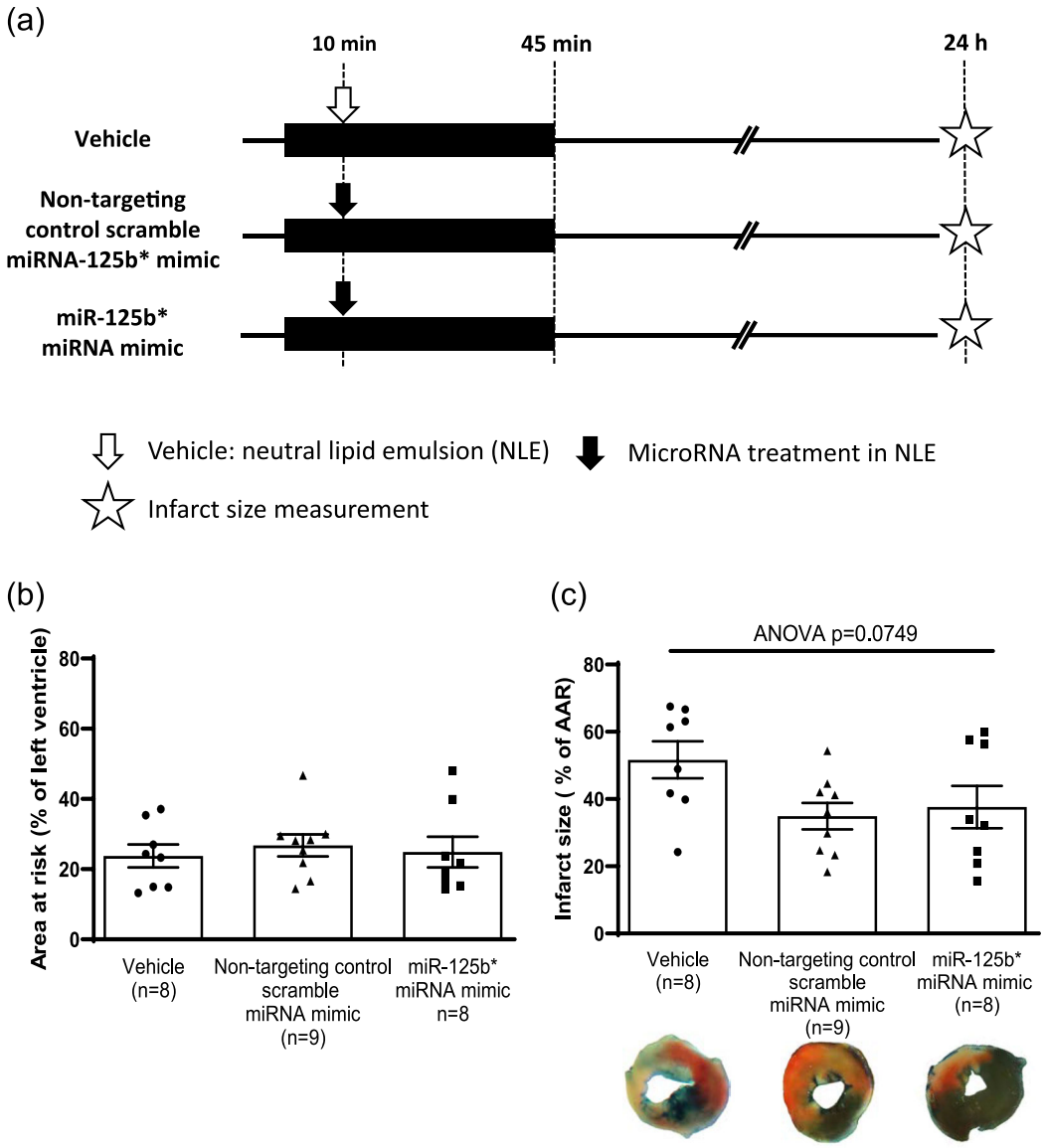

FIGURE 4 Proof-of-concept-1: *in vivo* acute myocardial infarction study. Experimental protocol of acute myocardial infarction (panel a), area at risk results (panel b) and infarct size results (panel c). Data are expressed as mean ± SEM, ordinary one-way ANOVA did not reach significance. Group sizes (n) as the number of animals are shown under the corresponding groups.

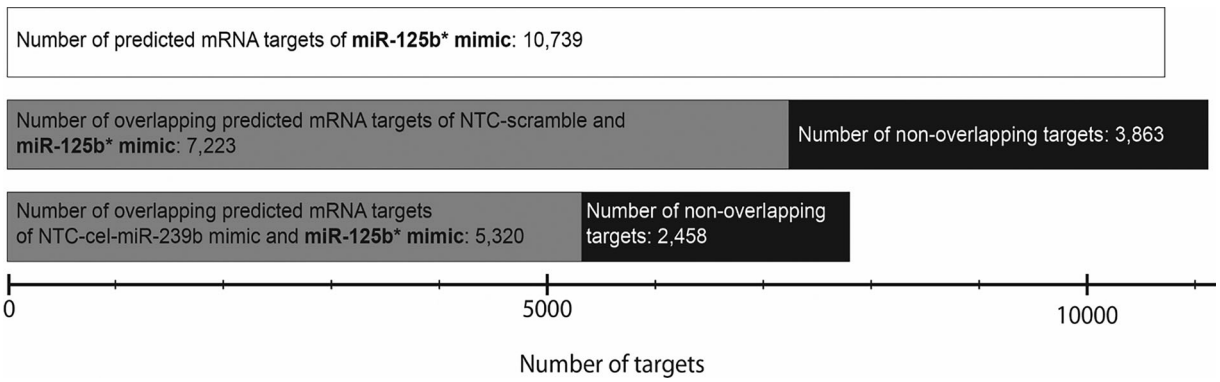

FIGURE 5 Scaled diagrams presenting overlapping target numbers between miR-125b* and the control miRNAs used in the studies. Target prediction was prepared considering predicted regulation either by guide, or passenger strand, or by both strands.

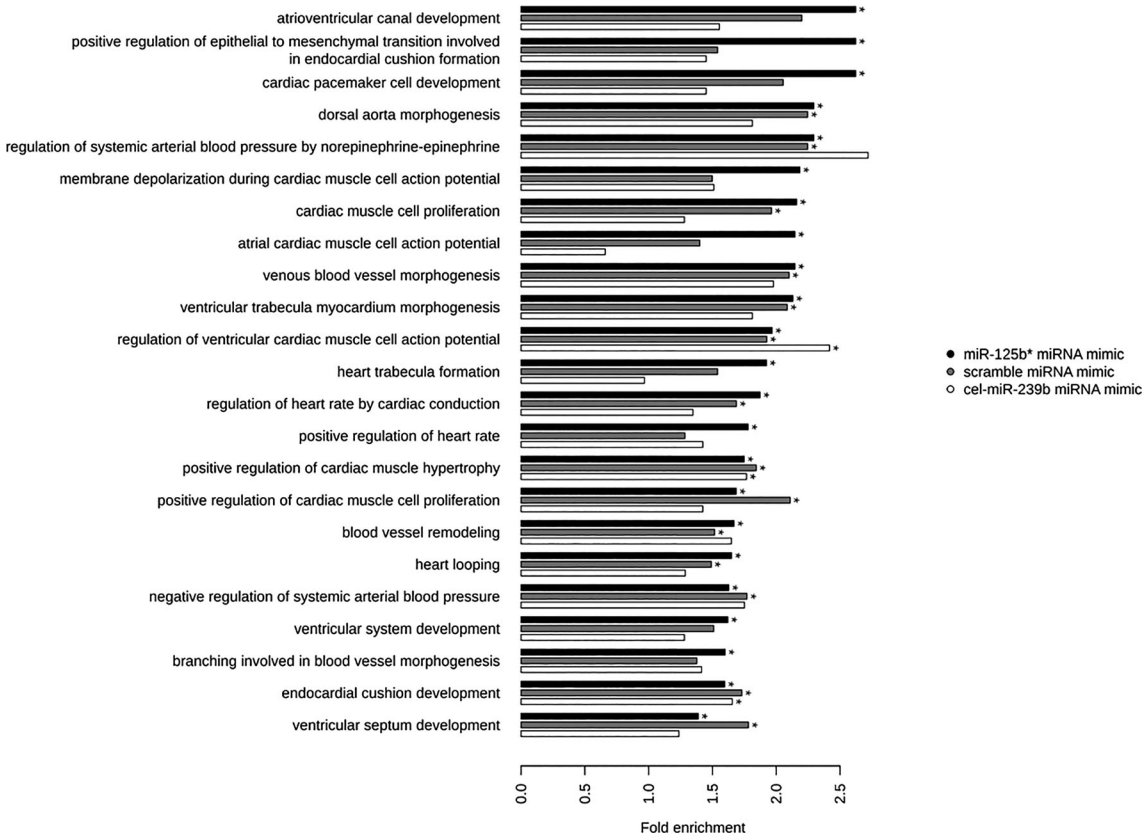

FIGURE 6 Enrichment results of selected most specific gene ontology biological process terms without any significantly enriched child term, identified as relative leaf terms, targeted by miR-125b* mimic in comparison with the enrichment results of scramble and cel-miR-239b mimic control. Over-representation analysis was performed with targets predicted to be regulated either by guide, or passenger strand, or by both strands of each sequence. Significant enrichment (FDR ≥ 0.05) is indicated with an asterisk.

3.2.3 | Effect of miR-125b* intravenous administration on infarct size (proof-of-concept study 2; PoC-2)

In PoC-2, we repeated the experiments of PoC-1 exchanging the scramble miRNA to cel-miR-239b as a non-targeting control miRNA derived from *C. elegans*, which is a commercially available miRNA used as a negative control (for experimental protocol see Figure 7, panel a). Other parameters and conditions were identical with PoC-1. In PoC-2 study, the size of area at risk (Figure 7, panel b) was also not significantly different between groups. We have found that miR-125b* mimic significantly reduced infarct size as compared with vehicle control and non-targeting cel-miR-239b had no effect on infarct size (Figure 7. panel c).

3.2.4 | All-cause mortality and incidence of arrhythmias in PoC-1 and -2 studies

All-cause mortality did not differ among experimental groups either in PoC-1 or in PoC-2 (see Table S7 for more details).

ECG was monitored during surgery and heart rate as well as the incidence of arrhythmias was analysed subsequently. There was no significant difference in either the heart rate (Table S8) or the incidence of arrhythmias (Table S9) occurring during 45 min of ischemia and the first 15 min of reperfusion at any time point between the groups, in either PoC studies.

3.2.5 | Principle component analysis

Principle component analysis of the RNA-sequencing data showed (Figure S2) that miR-125b* mimic treatment has only slight effect on the whole transcriptome.

3.3 | Assessing mechanism of action and target engagement of miR-125b* in the myocardium

We performed a specific and global second GO analysis to reveal the background molecular mechanisms of miR-125b*-evoked cardioprotection (for details, see Table S10 and Excel Sheet S1).

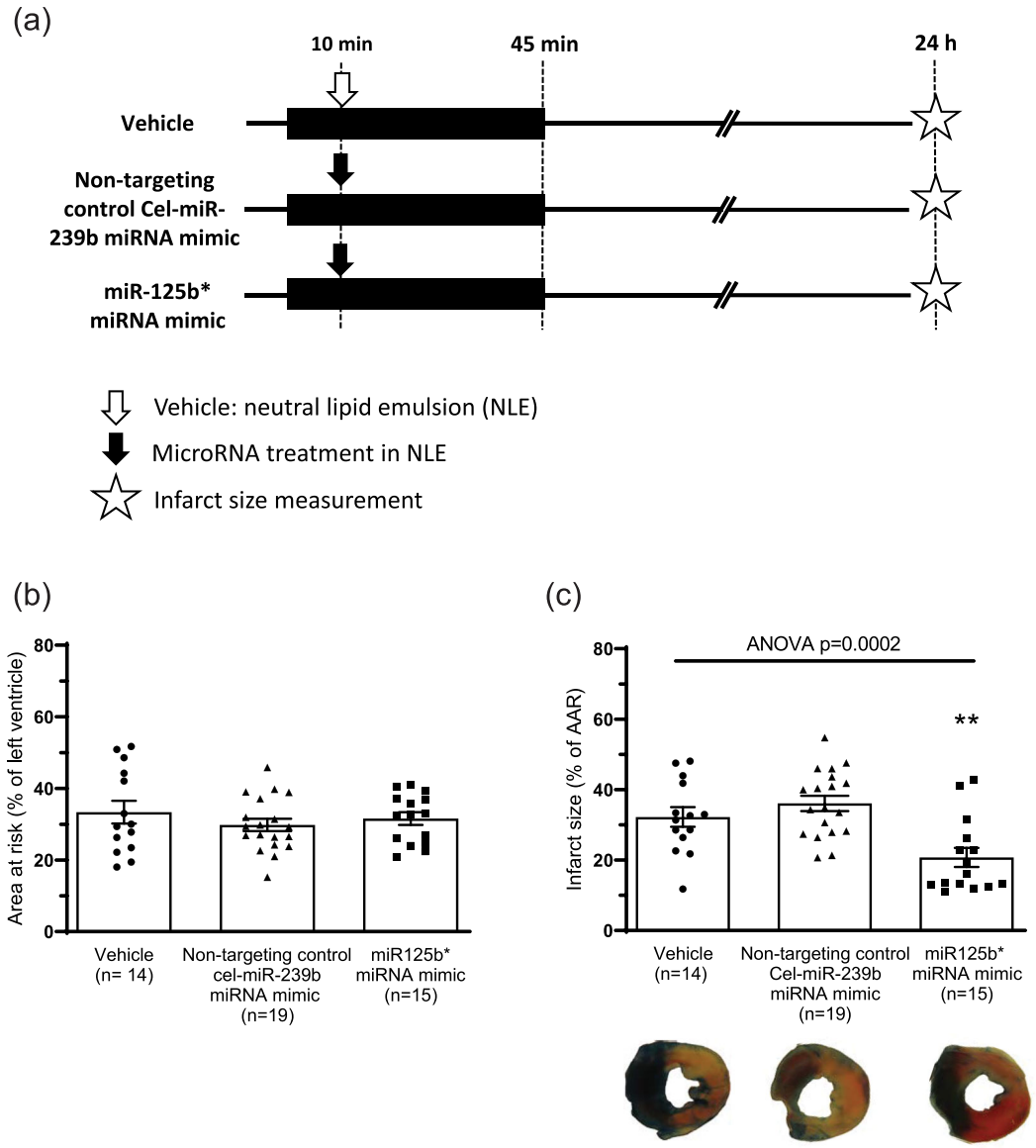

FIGURE 7 Proof of concept-2: *in vivo* acute myocardial infarction study. Experimental protocol of acute myocardial infarction (panel a), area at risk results of PoC-2 (panel b) and infarct size results of PoC-2 (panel c). Data are expressed as mean ± SEM, $^*P < 0.05$ versus vehicle, one-way ANOVA followed by Dunnett's post hoc test. Group sizes (n) as the number of animals are shown under the corresponding groups.

To further investigate the molecular mechanism of the cardioprotective effect of miR-125b* mimic and the alteration in the expression of its target genes, we determined cardiac expression of 5 selected targets, such as *Ccna2* and *Eef2k* selected from experimentally validated miRTarBASE database, as well as *Cacnb2*, *Kdm6a* and *Dab2* (Figure 8) selected from prediction-based databases according to the selection criteria detailed in the methodology chapter. Measurements with qRT-PCR was assessed 1, 2, 4, 8 or 24 h after a single intravenous administration of 10-μg miRNA-125b* mimic.

Target mRNA expression of *Ccna2*, *Eef2k* and *Cacnb2* showed a marked reduction 8 h after single intravenous miR-125b* mimic injection as compared with the time-matched vehicle, whereas mRNA expression of *Kdm6a* and *Dab2* were not significantly changed between groups at any time point (Figure 9).

4 | DISCUSSION

4.1 | Major findings and novelty of the study

This is the first report on the pharmacokinetic and pharmacodynamic properties of miR-125b* mimic after intravenous administration to intact mice. We found that miR-125b* expression was markedly increased in plasma and in the myocardium 1 h, as well as in liver

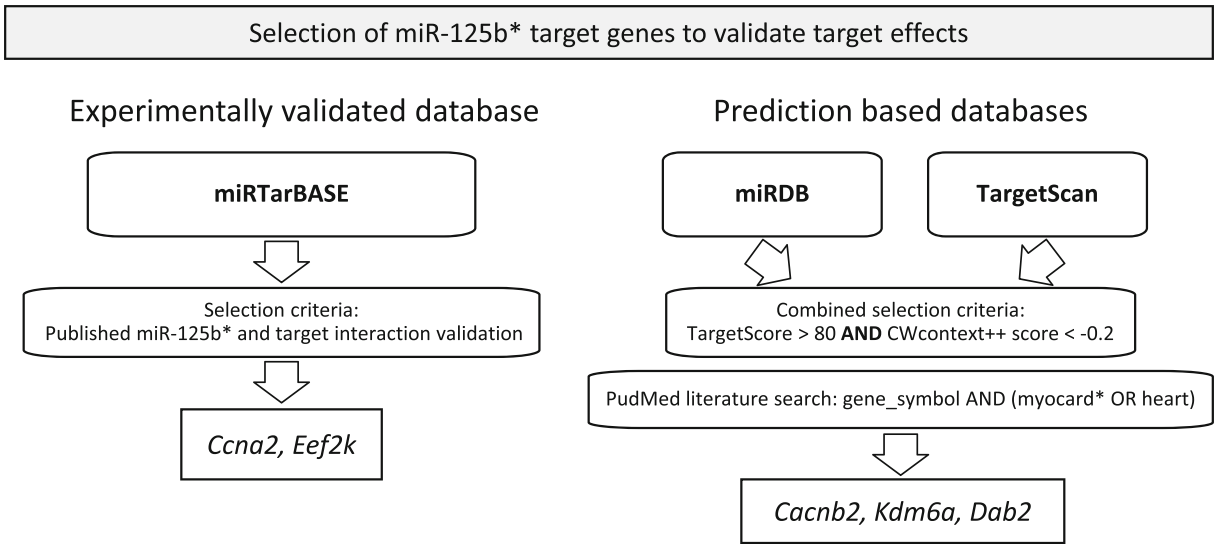

FIGURE 8 Selection of Ccnaa2 and *Eef2k* genes based on previous publications listed in miRTarBase database and selection of *Cacnb2*, *Kdm6a* and *Dab2* genes based on strong miRNA-target interaction prediction in the combination of two *in silico* predicted miRNA-target interaction databases (miRDB and TargetScan). Additionally, PubMed literature search was performed to filter the results of databases. Abbreviations:- Cyclin 2A (*Ccna2*); eukaryotic elongation factor-2 kinase (*Eef2k*); calcium voltage-gated channel auxiliary subunit beta 2 (*Cacnb2*); lysine (K)-specific demethylase 6A (*Kdm6a*); disabled homologue 2 (*Dab2*).

samples 2 h after i.v. bolus injection of 10 μg miR-125b* mimic. We have also shown first time that miR-125b* mimic administered intravenously during ischemia evoked cardioprotection by reducing infarct size significantly in an *in vivo* mouse model of acute myocardial infarction. We investigated the potential molecular mechanism of miR-125b* mimic-induced cardioprotection and found a significant downregulation of its target mRNAs such as *Ccna2* and *Eef2k* 8 h after its administration.

4.2 | Explorative pharmacokinetics

We have previously shown that cardiac expression of miR-125b* was counter-regulated after ischemic myocardial injury or cardiac ischemic pre- and postconditioning in isolated rat hearts. Furthermore, the cardioprotective effect of miR-125b* was confirmed by administration of its mimic to isolated neonatal cardiac myocytes subjected to simulated ischemia–reperfusion injury (Varga et al., 2014). However, the pharmacokinetic properties and *in vivo* proof of concept efficacy of miR-125b* mimic have yet to be investigated. Thus, we aimed to perform an explorative pharmacokinetic study with miR-125b* mimic and measured the relative expression of miR-125b* in plasma, heart, kidney and liver tissue samples after single intravenous administration of 10 μg of miRNA-125b* mimic. The expression of miR-125b* was increased in plasma and myocardial samples 1 h, and in the liver 2 h after administration comparing with time-matched vehicle control.

Although the number of publications investigating the function and biology of miRNAs is extensive, data on miRNA pharmacokinetics are severely limited. One of the first publications about miRNA mimic treatment showed that 3 days after intravenous injection of 80 mg·kg^{-1} miR-29b, its level was not different from that of saline-treated animals in any tissues including heart, lung, kidney and liver as determined by northern blot (van Rooij et al., 2008).

Recently, it has been published that a mixture of miR-302b/c/-367 mimics administered at 10 microg intravenous dose for mice reached the peak cardiac level between 4 and 8 h after administration and returned to baseline 24 h later (Tian et al., 2015). The authors showed a similar observation of miR-302 variants in the lung sample. The source of miRNA, that is, Dharmacon, Inc., as well as the vehicle, that is, neutral lipid emulsion, were identical with that we used in the present study.

Most recently, the pharmacokinetic properties of miR-144 mimic were determined after a single intravenous injection at 8 mg·kg^{-1} (Li et al., 2016). The authors measured miR-144 relative levels compared with miR control from plasma, heart, liver and kidney samples in a broader time scale from 1 h up to 28 days. Relative plasma levels of miR-144 increased to a 2.5-fold level 1 h after i.v. administration and remained around 2-fold elevated until 7 days. In the heart, miR-144 peak level was reached at 1.6-fold of control and remained slightly elevated (1.2-fold) until 14 days, then returned to baseline level. Except for one study (Wang et al., 2012), all other studies reported a similar distribution and elimination pattern of miRNA mimics, after administration of a single intravenous dose, in plasma and tissue samples to that we found in this study with miR-125b*. In the one exception, the authors used chemically modified miRNA mimics (Wang et al., 2012), which structural modification may prolong and enhance the presence of miRNAs in different tissues, especially in liver, kidney and spleen samples.

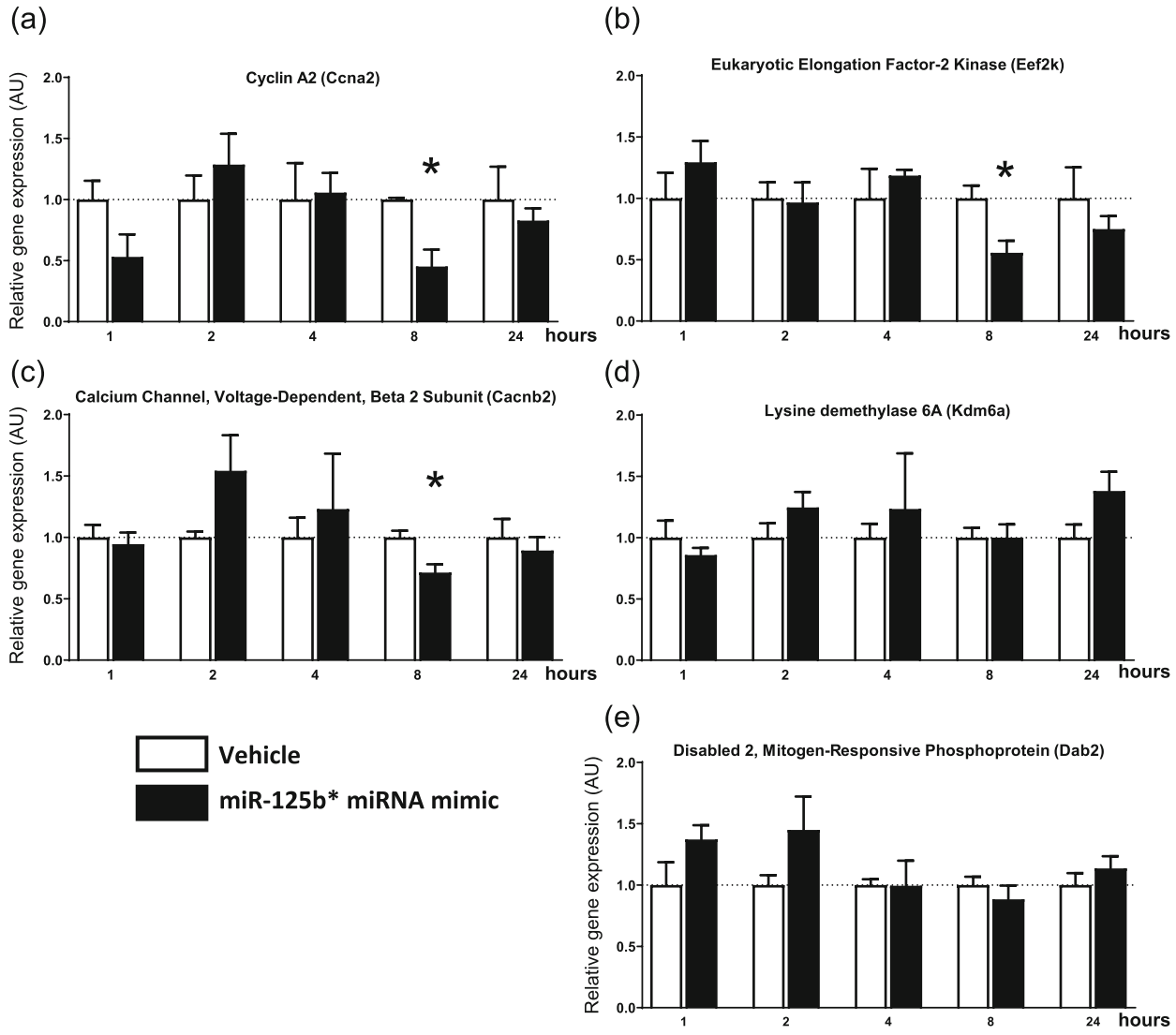

FIGURE 9 Relative cardiac mRNA expression of miR-125b* target genes in ratio to peptidylprolyl isomerase A (PPIA) control gene expression at different time points measured from ventricular samples. Data are expressed as mean ± SEM. *marked decrease without using any statistical analysis. Sample size of each group in each time point is indicated in Table S6, panel b. Panel a: Cyclin 2A (*Ccna2*); panel b: eukaryotic elongation factor-2 kinase (*Eef2k*); panel c: calcium voltage-gated channel auxiliary subunit beta 2 (*Cacnb2*); panel d: lysine (K)-specific demethylase 6A (*Kdm6a*); panel e: disabled homologue 2 (*Dab2*).

4.3 | Cardioprotection of miR-125b* mimic by reducing myocardial infarct size

The cardioprotective potential of miR-125b* (microRNA-125b-2-3p) against acute myocardial infarction was first suggested when we showed that its cardiac expression was decreased after myocardial ischemia–reperfusion injury and was counter-regulated by ischemic pre- and postconditioning. The cytoprotective effect of miR-125b* was also confirmed and biologically validated *in vitro* in neonatal rat cardiac myocytes subjected to simulated ischemia–reperfusion injury (Varga et al., 2014). In the present study, we further demonstrated the cardioprotective effect of miR-125b* by the reduction of myocardial infarct size after intravenous administration during ischemia in an *in vivo* mouse model of acute myocardial infarction.

In vivo cardioprotection by miR-125b has been shown by Wang et al. in 2014. However, there are several major differences between their and our present study: - (1) We used the matured sequence of miR-125b* containing 22 base pairs, whereas Wang and colleagues applied an unmatured oligonucleotide sequence of miR-125b consisting of 76 base pairs, although the sequence between 51 and 72 base pairs was identical with that we used in this study. (2) The way and the route of administration was also different. A lentiviral vector was used to transfect mouse hearts via an intra-arterial injection of pre-miR-125b containing mature miR-125b-5p and miR-125b-3p sequences and a stem loop, 7 days before a 45-min myocardial ischemia. (3) Finally, the time frame of follow-up was also different i.e. 4 h after the onset of reperfusion they found a reduced infarct size and decreased apoptosis by reduction in caspase 3, 7 and 8 activities, as

well as an improved cardiac function 3 and 7 days post-MI (Wang et al., 2014). The authors confirmed their finding in terms of infarct size reduction in a transgenic mouse model overexpressing miR-125b after 45-min ischemia and 24 h of reperfusion as compared with transgenic animals that received anti-miR-125 as an intracardiac injection into the anterior wall (Wang et al., 2014). The advance in our study is that we applied miR-125b* as a matured, short oligonucleotide sequence (as a miRNA mimic dissolved in neutral lipid emulsion) in a clinically more relevant intravenous route, administered during the time of myocardial ischemic injury.

4.4 | Coherence of the results in the cardioprotective effects of miR-125b family

The miR-125 family is highly conserved and it is composed of three homologues, that is, miR-125a, miR-125b-1 and miR-125b-2 both in humans and mice. MiR-125 family is implicated in a variety of physiological and pathological processes, including myocardial ischemia–reperfusion injury. MiR-125b* (miR-125b-2-3p) is a result of the maturation from miR-125b stem-loop sequence, as we summarized in our previous publication (Varga et al., 2018). However, miR-125 family members share the same conserved seed region (nucleotides 1–9), which suggests acting on several overlapping target molecules. Early studies with miR-125b overexpression constructed into a lentivirus-expressing system (Wang et al., 2014) or administration of exosomes abundant in miR-125b, derived from mesenchymal stem cells (Xiao et al., 2018), resulted in a significant decrease in myocardial infarct size and improvement of cardiac function in C57BL/6 mice subjected to myocardial ischemia–reperfusion injury. On the other hand, down-regulation of miR-125b was shown to induce cardiomyocyte apoptosis through activating the **p38-Sirt1**-p53 signalling pathway (Qiao et al., 2020). However, a contradictory preclinical study has shown that up-regulation of miR-125b may play a role in silencing **Cx43** and thereby may serve as a positive regulator of fibrotic remodelling in heart failure induced in **AMP-activated protein kinase α1 (PKAR1A)** knock out mice (Dufeys et al., 2021). There are also some concordant (Lv et al., 2021; Singh et al., 2020; Witten et al., 2022) as well as contradictory clinical data regarding the cardioprotective role of miR-125b (Gager et al., 2022; Jia et al., 2016). However, all clinical data are in association only with the circulating levels of miR-125b. Moreover, recently, circular RNAs, which may regulate the expression of miRNAs and the miRNA-mRNA signalling networks, have also been published to influence miR-125b expression in cardiovascular pathologies including acute myocardial infarction and myocardial ischemia–reperfusion injury (Luo et al., 2021; Wang, Li, et al., 2021; Wang, Sun, & Hu, 2021).

4.5 | Supposed molecular mechanism of action for cardioprotection evoked by miR-125b* mimic

As we discussed above, we used two experimentally validated targets, *Ccna2* and *Eef2k* for target validation of miR-125b* mimic. Both targets have previously been shown to be involved in the defence processes of macrophages, where both targets were down-regulated after overexpression of miR-125b-5p, which led to decreased **NO** production as well as to repression of **inducible NO synthase (iNOS)** in activated macrophages (Xu et al., 2016). Moreover, *Ccna2* have been shown to participate in the regenerative processes following myocardial infarction. The first, early report was on the potential involvement of cyclin A2 in mediating cardiomyocyte mitosis and thereby regeneration of the damaged myocardium (Chaudhry et al., 2004). Later on, left ventricular ejection fraction has been shown to be markedly enhanced in a transgenic mouse model of MI constitutively overexpressing myocardial cyclin A2 and subjected to permanent coronary ligation, 3 weeks as well as 3 months post-MI as compared with the non-transgenic animals (Cheng et al., 2007). Finally, Shapiro et al. have recently demonstrated that intramyocardial injections of adenoviral vectors containing murine cyclin A2 around the circumference of the peri-infarct zone 1 week after acute coronary occlusion in young female Yorkshire Landrace pigs, significantly increased LV ejection fraction and decreased collagen/muscle density 6 weeks after treatment as compared to the control animals (Shapiro et al., 2014). Although the direction of expression change in the above studies is opposite to the present study, the time scale of changes in cyclin A2 expression is markedly different in the two studies.

Regarding *Eef2k*, which is also involved in NO-related macrophage defence actions (see also above, [Xu et al., 2016]) and its detrimental role in cardiac autophagy processes (Kameshima et al., 2019) as well as in cardiac hypertrophy, which has been shown in several animal models, such as transverse aortic constriction (TAC)- and **isoprenaline**-induced hypertrophy (Kameshima et al., 2016). However, controversial role of *Eef2k* in cardiac cells was also recently shown in H9C2 cells subjected to glucose deprivation, where knockdown of *Eef2k* led to a decreased phosphorylation and thereby activation of *Eef2k*, which induced an increased rate of apoptotic cell death (Kameshima et al., 2019).

We have not found any literature in relation between *Cacnb2* and myocardial ischemia–reperfusion injury. However, data discussing its role in embryonal cardiac development (Chernyavskaya et al., 2012; Meissner et al., 2011) as well as its supposed function in cardiac remodelling during chronic heart failure models are available (Carrillo et al., 2011; MacDonnell et al., 2022).

5 | LIMITATIONS OF THE PRESENT STUDY

We did not determine mean arterial blood pressure and blood gas parameters during the *in vivo* experiments, which is a limitation of the 24-h surviving mouse model as arterial cannulation and blood sampling could highly increase mortality, respectively.

We did not measure markers of myocardial necrosis and microvascular obstruction because infarct size is a superior and more informative endpoint (Botker et al., 2018; Ferdinandy et al., 2023). We did not examine single-cell expression of miR-125b* in different cell types

of the heart. However, the available databases with single-cell gene and non-coding RNA expression contain incomplete miRNA data providing limited knowledge on cell specific expression profile of miRNAs.

The pharmacokinetics study was performed in control non-infarcted animals, although it cannot be excluded that the presence of myocardial infarction might alter the pharmacokinetics of miR-125b*. We determined renal, hepatic and cardiac, however not pulmonary expression of miR-125b* in the pharmacokinetics study, although lungs can affect the pharmacokinetics of miR-125b* mimic after iv. administration.

Finally, we used only male mice for the experiments, as premenopausal state in female animals (as well as in humans) is a cardioprotective state due to elevated plasma levels of estrogens, which has been shown in mice (Song et al., 2003) and in humans (Barrett-Connor, 1997), and extensively reviewed elsewhere (Knowlton & Korzick, 2014). Therefore, cardioprotection in female mice could be influenced by estrogens.

6 | CONCLUSIONS

This is the first explorative pharmacokinetic and molecular pharmacodynamic study on miR-125b* after its intravenous administration to intact mice. We found an increased plasma and cardiac expression of miR-125b* at 1 h, as well as a hepatic expression at 2 h after the single bolus administration of its mimic, and 8 h later the expression of its target mRNAs, such as *Ccna2*, *Eef2k* and *Cacnb2* were significantly down-regulated. We have also shown for the first time that miR-125b* mimic as a matured, short oligonucleotide sequence (dissolved in neutral lipid emulsion) administered as a single intravenous bolus during ischemia, evoked cardioprotection in terms of a significant decrease of myocardial infarct size in an *in vivo* mouse model of acute myocardial infarction. This model and experimental setup provides a clinically relevant scenario, which may have a high translational value to human disease, as well as it introduces further steps of miRNA-based cardioprotective drug development.

AUTHOR CONTRIBUTIONS

T. Szabados: Data curation (equal); investigation (equal); methodology (equal); writing—original draft (equal). **A. Makkos:** Conceptualization (equal); investigation (equal); methodology (equal); writing - original draft (equal). **B. Ágg:** Investigation (supporting); methodology (supporting); software (supporting); supervision (supporting); validation (supporting); visualization (supporting). **B. Benczik:** Methodology (supporting); software (supporting); visualization (supporting). **G. G. Brenner:** Conceptualization (supporting); methodology (supporting). **M. Szabó:** Formal analysis (equal). **B. Váradi:** Methodology (supporting); software (supporting); visualization (supporting). **I. Vörös:** Investigation (supporting); methodology (supporting). **K. Gömöri:** Investigation (supporting); methodology (supporting). **Z. V. Varga:** Conceptualization (supporting). **A. Görbe:** Conceptualization (supporting); data curation (lead); supervision (equal); validation (lead); writing—original draft (supporting). **P. Bencsik:** Conceptualization (equal); funding acquisition (supporting); investigation (equal); methodology (equal); supervision (equal); writing—original draft (lead). **P. Ferdinandy:** Conceptualization (lead); data curation (lead); funding acquisition (lead); supervision (lead).

ACKNOWLEDGEMENTS

The Ministry for Innovation and Technology in Hungary provided funding to this study under the Thematic Excellence Programme (2020-4.1.1.-TKP2020), the 2020-1.1.5-GYORSÍTÓSÁV call programme (2020-1.1.5-GYORSÍTÓSÁV-2021-00011), the TKP2021-EGA funding scheme (TKP2021-EGA-23) and the Research Excellence Programme (TKP/ITM/NKFIH). This study was also supported by Project no. RRF-2.3.1-21-2022-00003 'National Heart Laboratory, Hungary' implemented with the support provided by the European Union. This study was further supported by the National Research, Development and Innovation Office of Hungary (NKFIA; NVKP-16-1-2016-0017 National Heart Program). The research was further funded by the National Research, Development and Innovation Office of Hungary (NKFIA; VEKOP-2.3.2-16-2016-00002 and VEKOP-2.3.3-15-2017-00016 and the Hungarian National Scientific Research Fund [OTKA-138223]). T.Sz. was supported by the Cooperative Doctoral Programme (KDP-2020) of the Ministry for Innovation and Technology. MA was supported by ÚNKP-23-4-II-SE-34; New National Excellence Program of the Ministry for Innovation and Technology. P.B. (bo_481_21) was supported by the János Bolyai Research Scholarships of the Hungarian Academy of Sciences and by the ÚNKP-23-5-SZTE-704 New National Excellence Program of the Ministry of Human Capacities, as well as by the SZGYA2021 Grant of the Albert Szent-Györgyi Medical School of the University of Szeged.

CONFLICT OF INTEREST STATEMENT

P.F. and A.G. are inventors of the patent application of miR-125b* (WO 2013/057527). P.F. is the owner and CEO of Pharmahungary Ltd., where A.G., Z.G. and P.B. are employed as management staff. The other authors declare no conflict of interest.

DATA AVAILABILITY STATEMENT

The data that support the findings of this study are available from the corresponding author upon reasonable request. Some data may not be made available because of privacy or ethical restrictions.

DECLARATION OF TRANSPARENCY AND SCIENTIFIC RIGOUR

This declaration acknowledges that this paper adheres to the principles for transparent reporting and scientific rigour of preclinical research as stated in the BJP guidelines for Design and Analysis and Animal Experimentation, and as recommended by funding agencies, publishers and other organizations engaged with supporting research.

ORCID

Bence Ágg https://orcid.org/0000-0002-6492-0426
Bettina Benczik https://orcid.org/0000-0003-0379-2181
Imre Vörös https://orcid.org/0000-0001-5922-6109
Kamilla Gömöri https://orcid.org/0000-0001-9793-3138
Zoltán V. Varga https://orcid.org/0000-0002-2758-0784
Péter Bencsik https://orcid.org/0000-0003-1936-6232

REFERENCES

Agarwal, V., Bell, G. W., Nam, J. W., & Bartel, D. P. (2015). Predicting effective microRNA target sites in mammalian mRNAs. *eLife*, *4*. https://doi.org/10.7554/eLife.05005

Alexander, S. P. H., Fabbro, D., Kelly, E., Mathie, A. A., Peters, J. A., Veale, E. L., Armstrong, J. F., Faccenda, E., Harding, S. D., Davies, J. A., Annett, S., Boison, D., Burns, K. E., Dessauer, C., Gertsch, J., Helsby, N. A., Izzo, A. A., Ostrom, R., Papapetropoulos, A., … Wong, S. S. (2023). The Concise Guide to PHARMACOLOGY 2023/24: Enzymes. *British Journal of Pharmacology*, *180*(Suppl 2), S289–S373. https://doi.org/10.1111/bph.16181

Ashburner, M., Ball, C. A., Blake, J. A., Botstein, D., Butler, H., Cherry, J. M., & Sherlock, G. (2000). Gene ontology: Tool for the unification of biology. The gene ontology consortium. *Nature Genetics*, *25*(1), 25–29. https://doi.org/10.1038/75556

Barrett-Connor, E. (1997). Sex differences in coronary heart disease. Why are women so superior? The 1995 Ancel keys lecture. *Circulation*, *95*(1), 252–264. https://doi.org/10.1161/01.cir.95.1.252

Boengler, K., Kosiol, M., Mayr, M., Schulz, R., & Rohrbach, S. (2017). Mitochondria and ageing: Role in heart, skeletal muscle and adipose tissue. *Journal of Cachexia, Sarcopenia and Muscle*, *8*(3), 349–369. https://doi.org/10.1002/jcsm.12178

Botker, H. E., Hausenloy, D., Andreadou, I., Antonucci, S., Boengler, K., Davidson, S. M., & Heusch, G. (2018). Practical guidelines for rigor and reproducibility in preclinical and clinical studies on cardioprotection. *Basic Research in Cardiology*, *113*(5), 39. https://doi.org/10.1007/s00395-018-0696-8

Carbon, S., & Mungall, C. (2018). *Gene ontology data archive (2020-10-09) [data set]*. Zenodo. Retrieved from. https://doi.org/10.5281/zenodo.4081749

Carrillo, E. D., Escobar, Y., Gonzalez, G., Hernandez, A., Galindo, J. M., Garcia, M. C., & Sanchez, J. A. (2011). Posttranscriptional regulation of the beta2-subunit of cardiac L-type Ca2+ channels by MicroRNAs during long-term exposure to isoproterenol in rats. *Journal of Cardiovascular Pharmacology*, *58*(5), 470–478. https://doi.org/10.1097/FJC.0b013e31822a789b

Chaudhry, H. W., Dashoush, N. H., Tang, H., Zhang, L., Wang, X., Wu, E. X., & Wolgemuth, D. J. (2004). Cyclin A2 mediates cardiomyocyte mitosis in the postmitotic myocardium. *The Journal of Biological Chemistry*, *279*(34), 35858–35866. https://doi.org/10.1074/jbc.M404975200

Cheng, R. K., Asai, T., Tang, H., Dashoush, N. H., Kara, R. J., Costa, K. D., & Chaudhry, H. W. (2007). Cyclin A2 induces cardiac regeneration after myocardial infarction and prevents heart failure. *Circulation Research*, *100*(12), 1741–1748. https://doi.org/10.1161/CIRCRESAHA.107.153544

Chernyavskaya, Y., Ebert, A. M., Milligan, E., & Garrity, D. M. (2012). Voltage-gated calcium channel CACNB2 (beta2.1) protein is required in the heart for control of cell proliferation and heart tube integrity. *Developmental Dynamics*, *241*(4), 648–662. https://doi.org/10.1002/dvdy.23746

Conda Documentation. (n.d.) Retrieved from https://docs.conda.io/en/latest/

Csonka, C., Kupai, K., Kocsis, G. F., Novak, G., Fekete, V., Bencsik, P., & Ferdinandy, P. (2010). Measurement of myocardial infarct size in preclinical studies. *Journal of Pharmacological and Toxicological Methods*, *61*(2), 163–170. https://doi.org/10.1016/j.vascn.2010.02.014

Curtis, M. J., Alexander, S. P. H., Cirino, G., George, C. H., Kendall, D. A., Insel, P. A., Izzo, A. A., Ji, Y., Panettieri, R. A., Patel, H. H., Sobey, C. G., Stanford, S. C., Stanley, P., Stefanska, B., Stephens, G. J., Teixeira, M. M., Vergnolle, N., & Ahluwalia, A. (2022). Planning experiments: Updated guidance on experimental design and analysis and their reporting III. *British Journal of Pharmacology*, *179*(15), 3907–3913. https://doi.org/10.1111/bph.15868

Danecek, P., Bonfield, J. K., Liddle, J., Marshall, J., Ohan, V., Pollard, M. O., & Li, H. (2021). Twelve years of SAMtools and BCFtools. *GigaScience*, *10*(2). https://doi.org/10.1093/gigascience/giab008

Davidson, S. M., Ferdinandy, P., Andreadou, I., Botker, H. E., Heusch, G., Ibanez, B., & Action, C. C. (2019). Multitarget strategies to reduce myocardial ischemia/reperfusion injury: JACC review topic of the week. *Journal of the American College of Cardiology*, *73*(1), 89–99. https://doi.org/10.1016/j.jacc.2018.09.086

De Majo, F., & De Windt, L. J. (2018). RNA therapeutics for heart disease. *Biochemical Pharmacology*, *155*, 468–478. https://doi.org/10.1016/j.bcp.2018.07.037

Dufeys, C., Daskalopoulos, E. P., Castanares-Zapatero, D., Conway, S. J., Ginion, A., Bouzin, C., & Horman, S. (2021). AMPKalpha1 deletion in myofibroblasts exacerbates post-myocardial infarction fibrosis by a connexin 43 mechanism. *Basic Research in Cardiology*, *116*(1), 10. https://doi.org/10.1007/s00395-021-00846-y

Ewels, P., Magnusson, M., Lundin, S., & Kaller, M. (2016). MultiQC: Summarize analysis results for multiple tools and samples in a single report. *Bioinformatics*, *32*(19), 3047–3048. https://doi.org/10.1093/bioinformatics/btw354

Ferdinandy, P., Andreadou, I., Baxter, G. F., Botker, H. E., Davidson, S. M., Dobrev, D., & Schulz, R. (2023). Interaction of cardiovascular nonmodifiable risk factors, comorbidities and comedications with ischemia/reperfusion injury and cardioprotection by pharmacological treatments and ischemic conditioning. *Pharmacological Reviews*, *75*(1), 159–216. https://doi.org/10.1124/pharmrev.121.000348

Ferdinandy, P., Hausenloy, D. J., Heusch, G., Baxter, G. F., & Schulz, R. (2014). Interaction of risk factors, comorbidities, and comedications with ischemia/reperfusion injury and cardioprotection by preconditioning, postconditioning, and remote conditioning. *Pharmacological Reviews*, *66*(4), 1142–1174. https://doi.org/10.1124/pr.113.008300

Gager, G. M., Eyileten, C., Postula, M., Gasecka, A., Jarosz-Popek, J., Gelbenegger, G., & Siller-Matula, J. (2022). Association between the expression of MicroRNA-125b and survival in patients with acute coronary syndrome and coronary multivessel disease. *Frontiers in Cardiovascular Medicine*, *9*, 948006. https://doi.org/10.3389/fcvm.2022.948006

Gene Ontology Consortium. (2021). The gene ontology resource: Enriching a gold mine. *Nucleic Acids Research*, *49*(D1), D325–D334. https://doi.org/10.1093/nar/gkaa1113

Hanna, J., Hossain, G. S., & Kocerha, J. (2019). The potential for microRNA therapeutics and clinical research. *Frontiers in Genetics*, *10*, 478. https://doi.org/10.3389/fgene.2019.00478

Heger, J., Szabados, T., Brosinsky, P., Bencsik, P., Ferdinandy, P., & Schulz, R. (2023). Sex difference in cardioprotection against acute myocardial infarction in MAO-B knockout mice in vivo. *International Journal of Molecular Sciences*, *24*(7), 6443. https://doi.org/10.3390/ijms24076443

Huang, H. Y., Lin, Y. C., Cui, S., Huang, Y., Tang, Y., Xu, J., & Huang, H. D. (2022). miRTarBase update 2022: An informative resource for experimentally validated miRNA-target interactions. *Nucleic Acids Research*, *50*(D1), D222–D230. https://doi.org/10.1093/nar/gkab1079

Jia, K., Shi, P., Han, X., Chen, T., Tang, H., & Wang, J. (2016). Diagnostic value of miR-30d-5p and miR-125b-5p in acute myocardial infarction.

Molecular Medicine Reports, *14*(1), 184–194. https://doi.org/10.3892/mmr.2016.5246

Kameshima, S., Okada, M., Ikeda, S., Watanabe, Y., & Yamawaki, H. (2016). Coordination of changes in expression and phosphorylation of eukaryotic elongation factor 2 (eEF2) and eEF2 kinase in hypertrophied cardiomyocytes. *Biochemistry and Biophysics Reports*, *7*, 218–224. https://doi.org/10.1016/j.bbrep.2016.06.018

Kameshima, S., Okada, M., & Yamawaki, H. (2019). Eukaryotic elongation factor 2 (eEF2) kinase/eEF2 plays protective roles against glucose deprivation-induced cell death in H9c2 cardiomyoblasts. *Apoptosis*, *24*(3–4), 359–368. https://doi.org/10.1007/s10495-019-01525-z

Keller, A., Groger, L., Tschernig, T., Solomon, J., Laham, O., Schaum, N., & Ludwig, N. (2022). miRNATissueAtlas2: An update to the human miRNA tissue atlas. *Nucleic Acids Research*, *50*(D1), D211–D221. https://doi.org/10.1093/nar/gkab808

Kim, D., Langmead, B., & Salzberg, S. L. (2015). HISAT: A fast spliced aligner with low memory requirements. *Nature Methods*, *12*(4), 357–360. https://doi.org/10.1038/nmeth.3317

Kimura, R., Swarup, V., Tomiwa, K., Gandal, M. J., Parikshak, N. N., Funabiki, Y., & Hagiwara, M. (2019). Integrative network analysis reveals biological pathways associated with Williams syndrome. *Journal of Child Psychology and Psychiatry*, *60*(5), 585–598. https://doi.org/10.1111/jcpp.12999

Knowlton, A. A., & Korzick, D. H. (2014). Estrogen and the female heart. *Molecular and Cellular Endocrinology*, *389*(1–2), 31–39. https://doi.org/10.1016/j.mce.2014.01.002

Krützfeldt, J., Rajewsky, N., Braich, R., Rajeev, K. G., Tuschl, T., Manoharan, M., & Stoffel, M. (2005). Silencing of microRNAs in vivo with 'antagomirs'. *Nature*, *438*(7068), 685–689. https://doi.org/10.1038/nature04303

Li, H., Handsaker, B., Wysoker, A., Fennell, T., Ruan, J., Homer, N., & Genome Project Data Processing, S. (2009). The sequence alignment/map format and SAMtools. *Bioinformatics*, *25*(16), 2078–2079. https://doi.org/10.1093/bioinformatics/btp352

Li, J., Cai, S., Peng, J., Friedberg, M. K., & Redington, A. N. (2016). Time dependent distribution of MicroRNA 144 after intravenous delivery. *Microrna*, *5*(1), 36–49. https://doi.org/10.2174/2211536605666160322152146

Liao, Y., Smyth, G. K., & Shi, W. (2014). featureCounts: An efficient general purpose program for assigning sequence reads to genomic features. *Bioinformatics*, *30*(7), 923–930. https://doi.org/10.1093/bioinformatics/btt656

Love, M. I., Huber, W., & Anders, S. (2014). Moderated estimation of fold change and dispersion for RNA-seq data with DESeq2. *Genome Biology*, *15*(12), 550. https://doi.org/10.1186/s13059-014-0550-8

Luo, C., Ling, G. X., Lei, B. F., Feng, X., Xie, X. Y., Fang, C., & Zheng, B. S. (2021). Circular RNA PVT1 silencing prevents ischemia-reperfusion injury in rat by targeting microRNA-125b and microRNA-200a. *Journal of Molecular and Cellular Cardiology*, *159*, 80–90. https://doi.org/10.1016/j.yjmcc.2021.05.019

Lv, F., Liu, L., Feng, Q., & Yang, X. (2021). Long non-coding RNA MALAT1 and its target microRNA-125b associate with disease risk, severity, and major adverse cardiovascular event of coronary heart disease. *Journal of Clinical Laboratory Analysis*, *35*(4), e23593. https://doi.org/10.1002/jcla.23593

MacDonnell, S., Megna, J., Ruan, Q., Zhu, O., Halasz, G., Jasewicz, D., & Morton, L. (2022). Activin a directly impairs human cardiomyocyte contractile function indicating a potential role in heart failure development. *Frontiers in Cardiovascular Medicine*, *9*, 1038114. https://doi.org/10.3389/fcvm.2022.1038114

Makkos, A., Agg, B., Petrovich, B., Varga, Z. V., Gorbe, A., & Ferdinandy, P. (2021). Systematic review and network analysis of microRNAs involved in cardioprotection against myocardial ischemia/reperfusion injury and infarction: Involvement of redox signalling. *Free Radical Biology & Medicine*, *172*, 237–251. https://doi.org/10.1016/j.freeradbiomed.2021.04.034

McGeary, S. E., Lin, K. S., Shi, C. Y., Pham, T. M., Bisaria, N., Kelley, G. M., & Bartel, D. P. (2019). The biochemical basis of microRNA targeting efficacy. *Science*, *366*(6472). https://doi.org/10.1126/science.aav1741

Meissner, M., Weissgerber, P., Londono, J. E., Prenen, J., Link, S., Ruppenthal, S., & Flockerzi, V. (2011). Moderate calcium channel dysfunction in adult mice with inducible cardiomyocyte-specific excision of the cacnb2 gene. *The Journal of Biological Chemistry*, *286*(18), 15875–15882. https://doi.org/10.1074/jbc.M111.227819

Pearson, K. (1901). LIII. On lines and planes of closest fit to systems of points in space. *The London, Edinburgh, and Dublin Philosophical Magazine and Journal of Science*, *2*(11), 559–572. https://doi.org/10.1080/14786440109462720

Percie du Sert, N., Hurst, V., Ahluwalia, A., Alam, S., Avey, M. T., Baker, M., & Wurbel, H. (2020). The ARRIVE guidelines 2.0: Updated guidelines for reporting animal research. *PLoS Biology*, *18*(7), e3000410. https://doi.org/10.1371/journal.pbio.3000410

Qiao, G. H., Zhu, P., Yue, L., & Yue, S. (2020). MiR-125b improves acute myocardial infarction in rats by regulating P38/Sirtl/P53 signaling pathway. *Journal of Biological Regulators and Homeostatic Agents*, *34*(4), 1297–1306. https://doi.org/10.23812/20-177-A

R Core Team. (2018). R: A language and environment for statistical computing. Retrieved from https://www.R-project.org/

Roberts, T. C., Langer, R., & Wood, M. J. A. (2020). Advances in oligonucleotide drug delivery. *Nature Reviews. Drug Discovery*, *19*(10), 673–694. https://doi.org/10.1038/s41573-020-0075-7

Sayour, N. V., Brenner, G. B., Makkos, A., Kiss, B., Kovacshazi, C., Gergely, T. G., & Giricz, Z. (2023). Cardioprotective efficacy of limb remote ischaemic preconditioning in rats: Discrepancy between a meta-analysis and a three-Centre in vivo study. *Cardiovascular Research*, *119*(6), 1336–1351. https://doi.org/10.1093/cvr/cvad024

Shapiro, S. D., Ranjan, A. K., Kawase, Y., Cheng, R. K., Kara, R. J., Bhattacharya, R., & Chaudhry, H. W. (2014). Cyclin A2 induces cardiac regeneration after myocardial infarction through cytokinesis of adult cardiomyocytes. *Science Translational Medicine*, *6*(224), 227. https://doi.org/10.1126/scitranslmed.3007668

Singh, S., de Ronde, M. W. J., Kok, M. G. M., Beijk, M. A., de Winter, R. J., van der Wal, A. C., & Pinto-Sietsma, S. J. (2020). MiR-223-3p and miR-122-5p as circulating biomarkers for plaque instability. *Open Heart*, *7*(1). https://doi.org/10.1136/openhrt-2019-001223

Song, X., Li, G., Vaage, J., & Valen, G. (2003). Effects of sex, gonadectomy, and oestrogen substitution on ischaemic preconditioning and ischaemia-reperfusion injury in mice. *Acta Physiologica Scandinavica*, *177*(4), 459–466. https://doi.org/10.1046/j.1365-201X.2003.01068.x

Tabula Muris, C. (2020). A single-cell transcriptomic atlas characterizes ageing tissues in the mouse. *Nature*, *583*(7817), 590–595. https://doi.org/10.1038/s41586-020-2496-1

Tabula Muris, C., Overall, C., Logistical, C., Organ, C., Processing Library, P., & Principal, I. (2018). Single-cell transcriptomics of 20 mouse organs creates a Tabula Muris. *Nature*, *562*(7727), 367–372. https://doi.org/10.1038/s41586-018-0590-4

Tian, Y., Liu, Y., Wang, T., Zhou, N., Kong, J., Chen, L., & Morrisey, E. E. (2015). A microRNA-hippo pathway that promotes cardiomyocyte proliferation and cardiac regeneration in mice. *Science Translational Medicine*, *7*(279), 279ra238. https://doi.org/10.1126/scitranslmed.3010841

Uhlmann, S., Mannsperger, H., Zhang, J. D., Horvat, E. A., Schmidt, C., Kublbeck, M., & Sahin, O. (2012). Global microRNA level regulation of EGFR-driven cell-cycle protein network in breast cancer. *Molecular Systems Biology*, *8*, 570. https://doi.org/10.1038/msb.2011.100

van Rooij, E., Sutherland, L. B., Thatcher, J. E., DiMaio, J. M., Naseem, R. H., Marshall, W. S., & Olson, E. N. (2008). Dysregulation of

microRNAs after myocardial infarction reveals a role of miR-29 in cardiac fibrosis. *Proceedings of the National Academy of Sciences of the United States of America*, *105*(35), 13027–13032. https://doi.org/10.1073/pnas.0805038105

Varga, Z. V., Agg, B., & Ferdinandy, P. (2018). miR-125b is a protectomiR: A rising star for acute cardioprotection. *Journal of Molecular and Cellular Cardiology*, *115*, 51–53. https://doi.org/10.1016/j.yjmcc.2017.12.010

Varga, Z. V., Zvara, A., Farago, N., Kocsis, G. F., Pipicz, M., Gaspar, R., & Ferdinandy, P. (2014). MicroRNAs associated with ischemia-reperfusion injury and cardioprotection by ischemic pre- and postconditioning: ProtectomiRs. *American Journal of Physiology. Heart and Circulatory Physiology*, *307*(2), H216–H227. https://doi.org/10.1152/ajpheart.00812.2013

Wang, H., Chiu, M., Xie, Z., Chiu, M., Liu, Z., Chen, P., & Chan, K. K. (2012). Synthetic microRNA cassette dosing: Pharmacokinetics, tissue distribution and bioactivity. *Molecular Pharmaceutics*, *9*(6), 1638–1644. https://doi.org/10.1021/mp2006483

Wang, S., Li, L., Deng, W., & Jiang, M. (2021). CircRNA MFACR is upregulated in myocardial infarction and downregulates miR-125b to promote cardiomyocyte apoptosis induced by hypoxia. *Journal of Cardiovascular Pharmacology*, *78*(6), 802–808. https://doi.org/10.1097/FJC.0000000000001123

Wang, X., Ha, T., Zou, J., Ren, D., Liu, L., Zhang, X., & Li, C. (2014). MicroRNA-125b protects against myocardial ischaemia/reperfusion injury via targeting p53-mediated apoptotic signalling and TRAF6. *Cardiovascular Research*, *102*(3), 385–395. https://doi.org/10.1093/cvr/cvu044

Wang, X., Sun, Q., & Hu, W. (2021). Carvedilol protects against the H2O2-induced cell damages in rat myoblasts by regulating the Circ_NFIX/miR-125b-5p/TLR4 signal Axis. *Journal of Cardiovascular Pharmacology*, *78*(4), 604–614. https://doi.org/10.1097/FJC.0000000000001095

Williams, C. R., Baccarella, A., Parrish, J. Z., & Kim, C. C. (2016). Trimming of sequence reads alters RNA-Seq gene expression estimates. *BMC Bioinformatics*, *17*, 103. https://doi.org/10.1186/s12859-016-0956-2

Winkle, M., El-Daly, S. M., Fabbri, M., & Calin, G. A. (2021). Noncoding RNA therapeutics - challenges and potential solutions. *Nature Reviews. Drug Discovery*, *20*(8), 629–651. https://doi.org/10.1038/s41573-021-00219-z

Witten, A., Martens, L., Schafer, A. C., Troidl, C., Pankuweit, S., Vlacil, A. K., & Markus, B. (2022). Monocyte subpopulation profiling indicates CDK6-derived cell differentiation and identifies subpopulation-specific miRNA expression sets in acute and stable coronary artery disease. *Scientific Reports*, *12*(1), 5589. https://doi.org/10.1038/s41598-022-08600-7

Wong, N., & Wang, X. (2015). miRDB: An online resource for microRNA target prediction and functional annotations. *Nucleic Acids Research*, *43*(Database issue), D146–D152. https://doi.org/10.1093/nar/gku1104

Xiao, C., Wang, K., Xu, Y., Hu, H., Zhang, N., Wang, Y., & Hu, X. (2018). Transplanted mesenchymal stem cells reduce autophagic flux in infarcted hearts via the exosomal transfer of miR-125b. *Circulation Research*, *123*(5), 564–578. https://doi.org/10.1161/CIRCRESAHA.118.312758

Xu, Z., Zhao, L., Yang, X., Ma, S., Ge, Y., Liu, Y., & Zheng, D. (2016). Mmu-miR-125b overexpression suppresses NO production in activated macrophages by targeting eEF2K and CCNA2. *BMC Cancer*, *16*, 252. https://doi.org/10.1186/s12885-016-2288-z

Yu, G., Wang, L. G., Han, Y., & He, Q. Y. (2012). clusterProfiler: An R package for comparing biological themes among gene clusters. *Omics*, *16*(5), 284–287. https://doi.org/10.1089/omi.2011.0118

SUPPORTING INFORMATION

Additional supporting information can be found online in the Supporting Information section at the end of this article.

How to cite this article: Szabados, T., Makkos, A., Ágg, B., Benczik, B., Brenner, G. G., Szabó, M., Váradi, B., Vörös, I., Gömöri, K., Varga, Z. V., Görbe, A., Bencsik, P., & Ferdinandy, P. (2025). Pharmacokinetics and cardioprotective efficacy of intravenous miR-125b* microRNA mimic in a mouse model of acute myocardial infarction. *British Journal of Pharmacology*, *182*(2), 432–450. https://doi.org/10.1111/bph.17345